Supplementary Information for

Single-crystal-to-single-crystal guest exchange in columnar assembled brominated triphenylamine *bis*-urea macrocycles

Ammon J. Sindt,[a] Mark D. Smith, [a] Samuel Berens,[b] Sergey Vasenkov, [b] Clifford R. Bowers, [c] and Linda S. Shimizu [a] *

[a] Department of Chemistry and Biochemistry, University of South Carolina, Columbia, SC 29208.

[b] Department of Chemical Engineering, University of Florida, Gainesville, FL 32611.

[c] Department of Chemistry, University of Florida, Columbia, Gainesville, FL 32611.

**E-mail:* SHIMIZLS@mailbox.sc.edu

Contents

General experimental

NMR spectra were recorded on Bruker 300 or 400 MHz spectrometers. Chemical shifts are reported in ppm (δ) and were internally referenced with the solvent peak. All chemicals were purchased from chemical suppliers and were used as received unless otherwise noted. High-resolution mass spectrum data were recorded using a direct exposure probe (DEP) in electron ionization mode on a Waters QTOF-I quadrupole time-of-flight mass spectrometer. All other instrument protocols are described in their own sections hereafter.

Synthesis and characterization of linear analogs and macrocycles

Scheme S1. Overview of synthesis of linear analogs and macrocycles

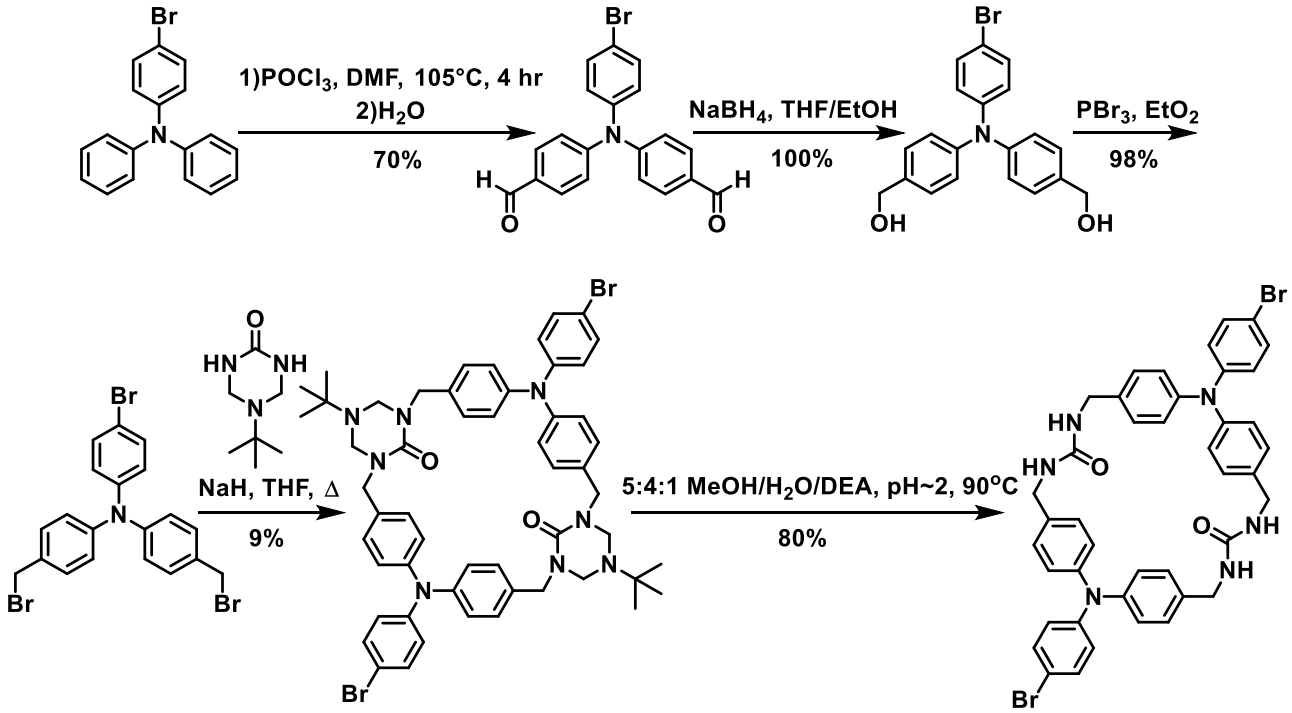

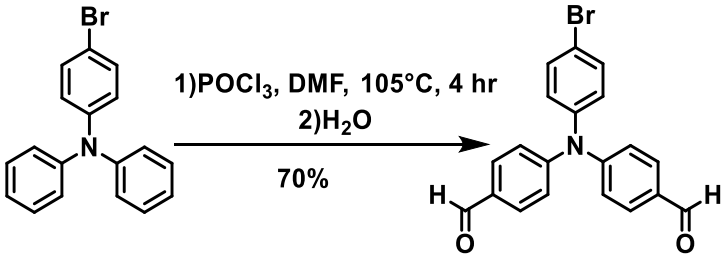

4,4'-((4-Bromophenyl)azanediyl)dibenzaldehyde: Phosphoryl chloride (10.00 mL, 107.3 mmol) was added dropwise to dry *N, N*-dimethylformamide (10.80 mL, 139.4 mmol) under nitrogen and the mixture was stirred at room temperature for one hour. Then 4-bromo-*N, N*-diphenylaniline (3.48 g, 10.7 mmol) was added, and this mixture stirred for 4 hours at 105 ˚C. After the mixture cooled to room temperature, 110 mL of ice-cold water was added to the mixture and it was filtered. The crude product was purified by column chromatography (Hexanes/Diethyl Ether = 3:1) to yield the product as a yellow solid (70%). Spectra matched that as previously reported.[1] ^{1}H NMR (300 MHz, $CDCl_3$): δ (ppm) 9.90 (s, 2H), 7.79 (d, *J* = 8.6 Hz, 4H), 7.50 (d, *J* = 8.9 Hz, 2H), 7.18 (d, *J* = 8.6 Hz, 4H), 7.05 (d, *J* = 8.6 Hz, 2H).

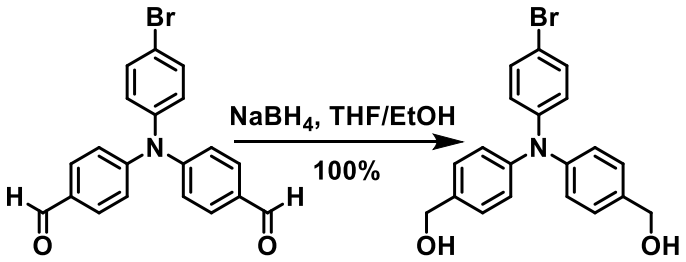

(((4-Bromophenyl)azanediyl)*bis*(4,1-phenylene))dimethanol: The previous aldehyde (1.724 g, 4.5 mmol) and sodium borohydride (0.378 g, 10.0 mmol) were suspended in 120 mL of a 2:1 mixture of dry tetrahydrofuran and ethanol and was heated at 40 ˚C overnight in the dark. Then the reaction was cooled to room temperature and 120 mL of water was added to quench the reaction. The mixture was extracted with chloroform (3 x 120 mL) and dried with $NaSO_4$. The solvent was removed under rotary evaporation yielding the product as a white solid (100%). ^{1}H NMR (300 MHz, $(CD_3)_2SO$): δ (ppm) 7.40 (d, *J* = 8.8 Hz, 2H), 7.26 (d, *J* = 8.3 Hz, 4H), 6.98 (d, *J* = 8.6 Hz, 4H), 6.84 (d, *J* = 9 Hz, 2H), 5.13 (t, *J* = 5.8 Hz, 2H), 4.44 (d, *J* = 5.7 Hz, 4H). ^{13}C NMR (75 MHz, $(CD_3)_2SO$): δ (ppm) 147.01, 145.41, 137.92, 132.04, 127.94, 124.21, 123.81, 113.14, 62.53. HRMS (DEP): [M+] calculated, 384.0594; found, 384.0593.

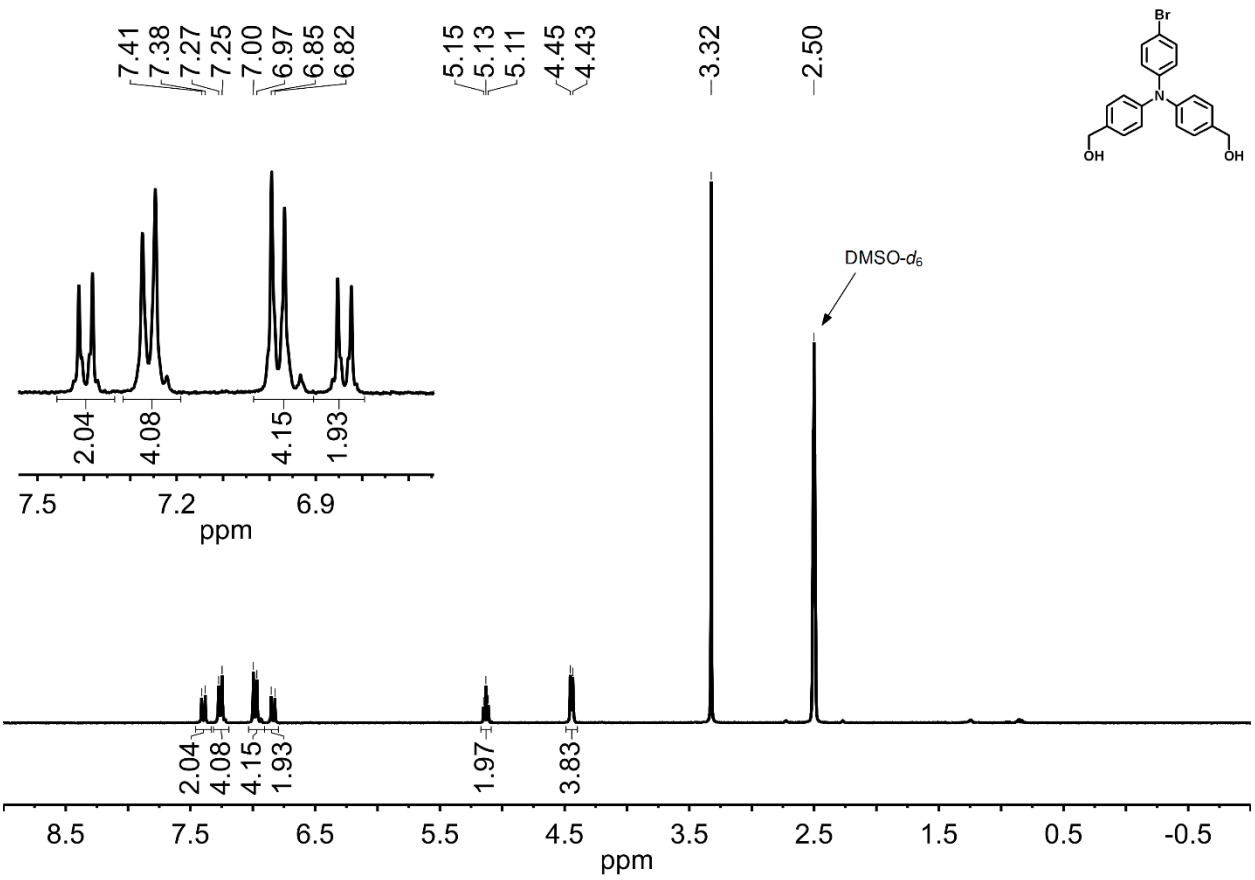

Figure S1. ^{1}H NMR ($(CD_3)_2SO$, 300 MHz)

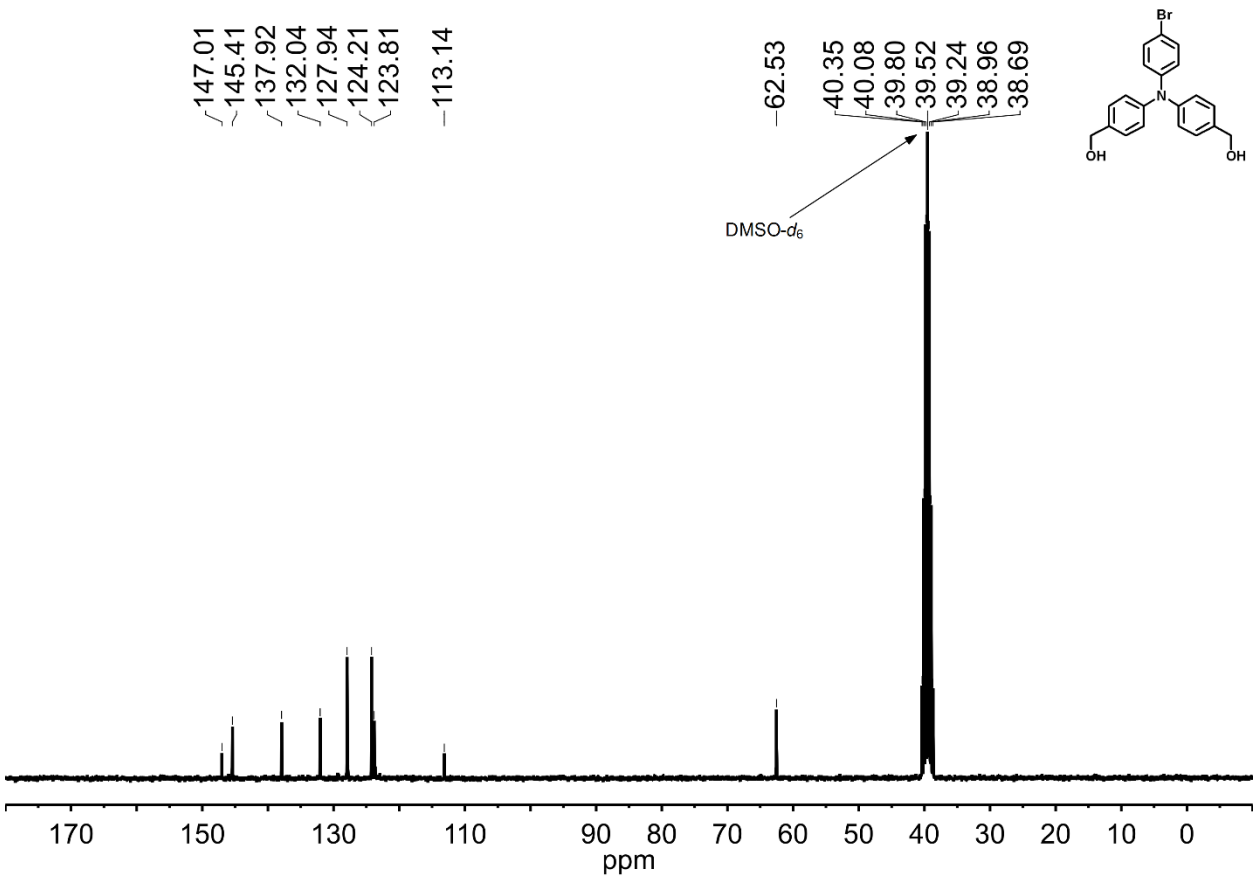

Figure S2. ^{13}C NMR ($(CD_3)_2SO$, 75 MHz)

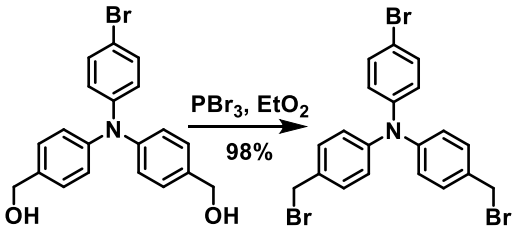

4-Bromo-*N*,*N*-*bis*(4-(bromomethyl)phenyl)aniline: The previous alcohol (1.733 g, 4.5 mmol) was suspended in 50 mL of dry diethyl ether and was cooled to 0 ˚C. Then a solution of phosphorus tribromide (514 µL, 5.4 mmol) in 10 mL dry diethyl ether was added dropwise over 5 minutes. The reaction stirred at room temperature overnight in the dark. In the morning, 60 and 30 mL of ice cold water and saturated $NaHCO_{3(aq)}$ was added to quench the reaction. The mixture was extracted with 60 mL of dichloromethane and the organics were washed with brine (3 x 60 mL) and dried with $MgSO_4$. The solvent was removed under rotary evaporation to yield the bromide as a sticky solid (98%). ^{1}H NMR (300 MHz, CD_2Cl_2): δ (ppm) 7.38 (d, *J* = 8.6 Hz, 2H), 7.29 (d, *J* = 8.6 Hz, 4H), 7.02 (d, *J* = 8.6 Hz, 4H), 6.97 (d, *J* = 8.6 Hz, 2H), 4.51 (s, 4H). ^{13}C NMR (75 MHz, CD_2Cl_2): δ (ppm) 147.55, 146.68, 133.03, 132.80, 130.68, 126.65, 124.36, 116.38, 34.25. HRMS (DEP): [M+] calculated, 506.8833; found, 506.8837.

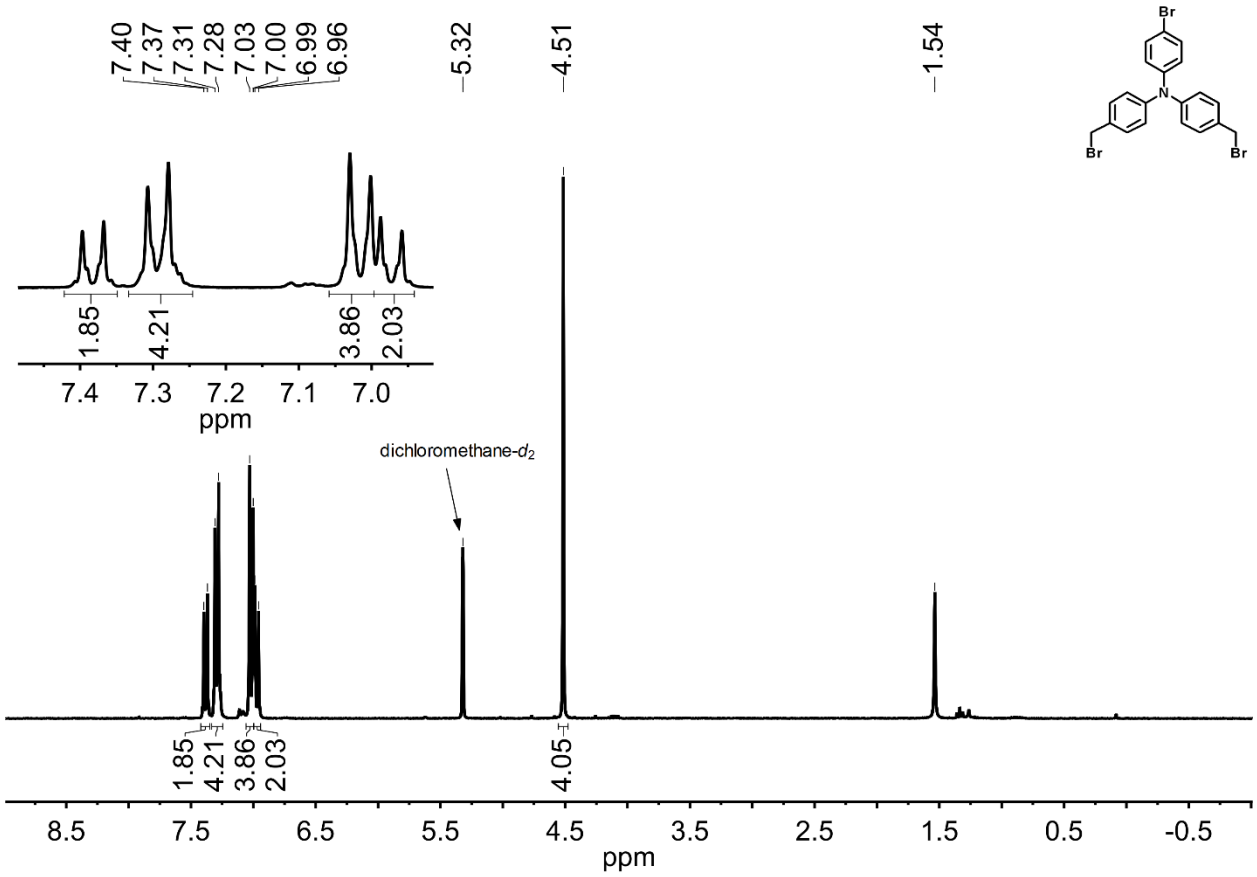

Figure S3. ^{1}H NMR (CD_2Cl_2, 300 MHz)

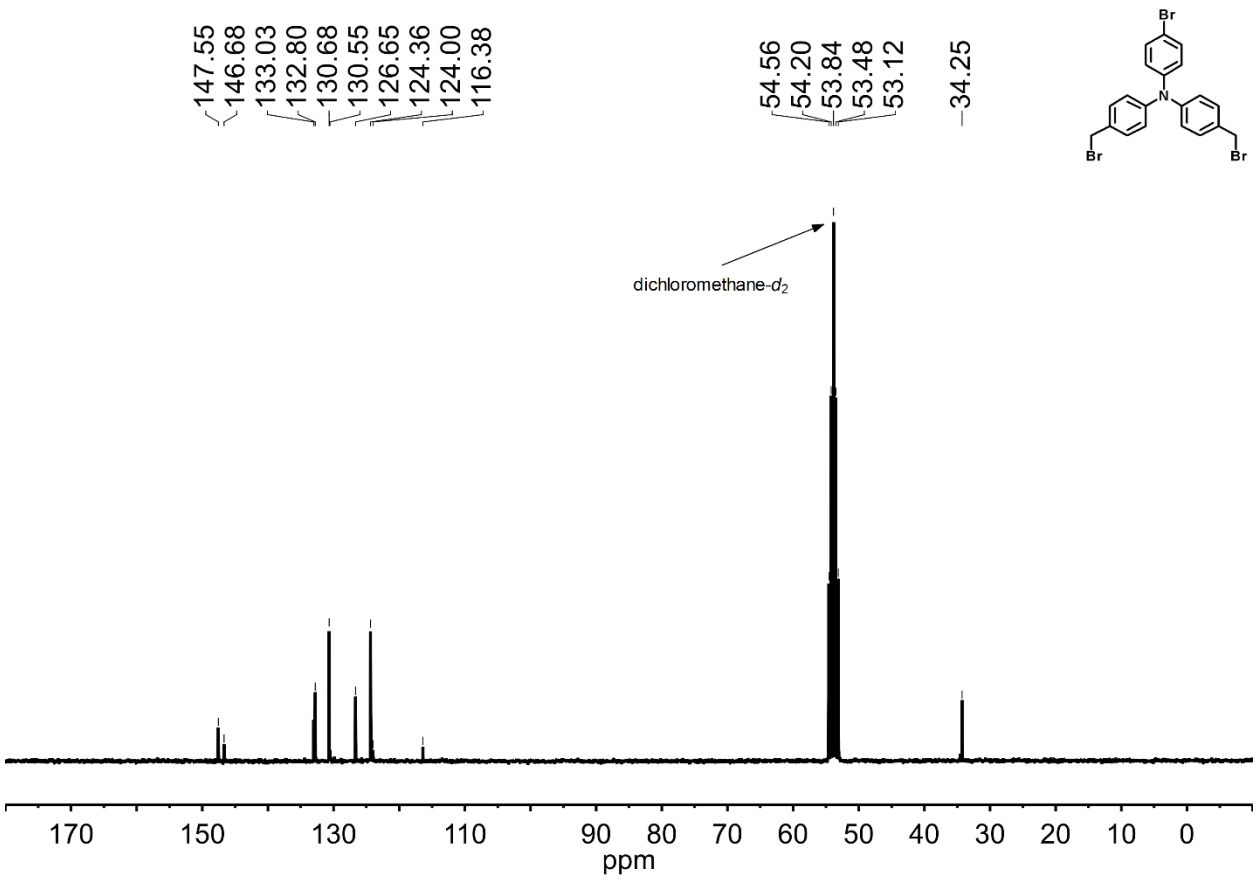

Figure S4. ^{13}C NMR (CD_2Cl_2, 75 MHz)

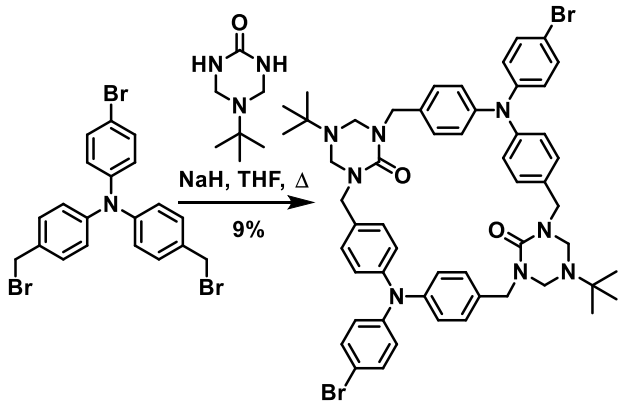

4,10-*bis*(4-Bromophenyl)-1^5,7^5-di-*tert*-butyl-4,10-diaza-1,7(1,3)-ditriazinana-3,5,9,11(1,4)-tetrabenzenacyclododecaphane-1^2,7^2-dione: *tert*-Butyl triazinanone (1.321 g, 8.4 mmol) and sodium hydride (60% suspension in paraffin oil, 1.344 g, 33.6 mmol) were suspended in 330 mL of dry tetrahydrofuran and was stirred for 2 hours at reflux. After cooling to room temperature, the previous bromide (4.285 g, 8.4 mmol) was added as a solution in 330 mL of dry tetrahydrofuran. The reaction stirred at reflux in the dark for 2 days. Upon completion, the reaction was quenched with 17 and 61 mL of 1N $HCl_{(aq)}$ and water then reduced *in vacuo* to 330 mL. An additional 44 and 218 mL of 1N $HCl_{(aq)}$ and water were added to the solution before it was extracted with dichloromethane (3 x 440 mL). The combined organic layers were washed with brine (1 x 440 mL) and dried with $MgSO_4$. The solvent was removed via rotary evaporation, and then the material was recrystallized from chloroform. Vacuum drying the crystals yielded the product as a white powder (9%). ^{1}H NMR (400 MHz, TCE-d_2, 90˚C): δ (ppm) 7.39 (d, *J* = 8.7 Hz, 4H), 7.25 (d, 8.1 Hz, 8H), 7.03 (m, 12H), 4.46 (br, 8H), 4.29 (s, 8H), 0.83 (s, 18H). ^{13}C NMR (75 MHz, $CDCl_3$): δ (ppm) 155.59, 147.03, 146.70, 133.02, 132.35, 130.58, 125.34, 124.23, 115.14, 60.29, 54.46, 47.07, 28.30. HRMS (DEP): [M+] calculated, 1009.3122; found, 1009.3136.

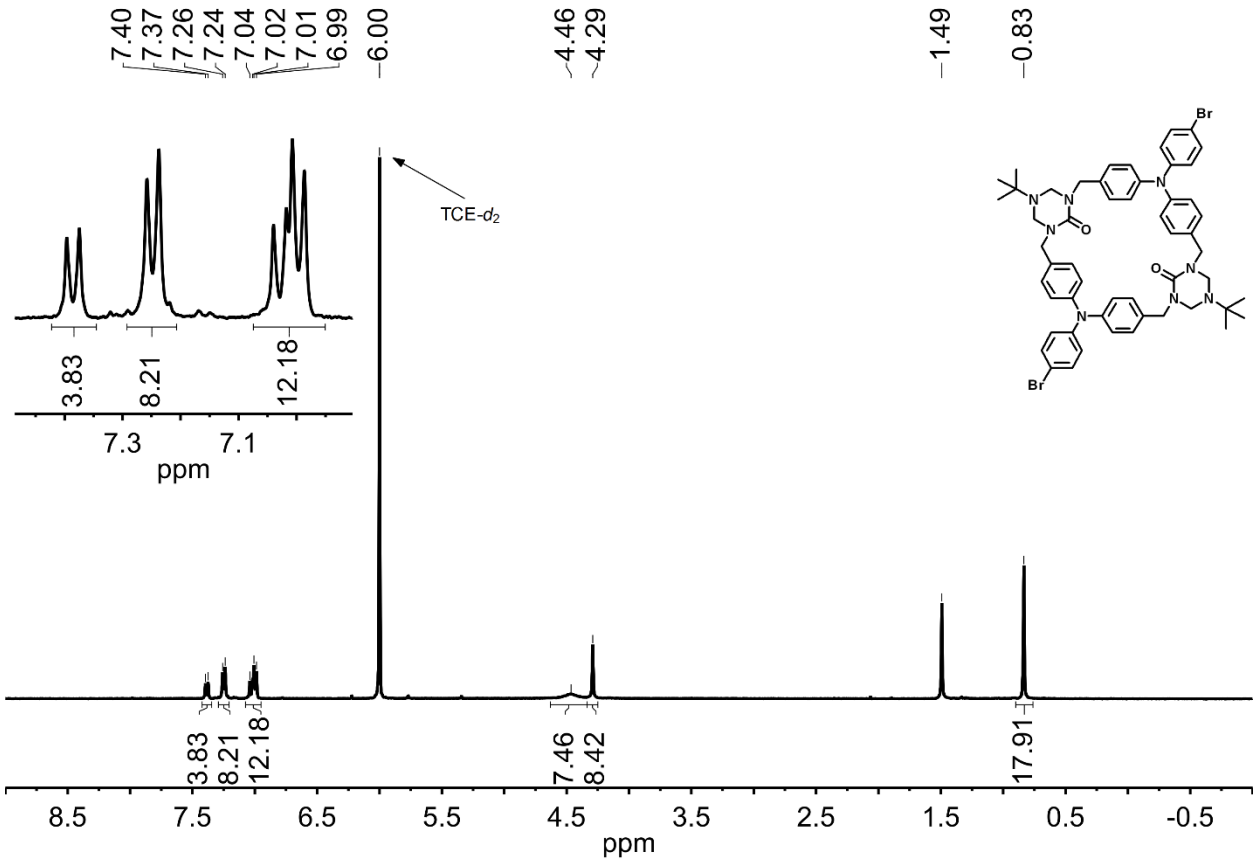

Figure S5. ^{1}H NMR (TCE-d_2, 90˚C, 400 MHz)

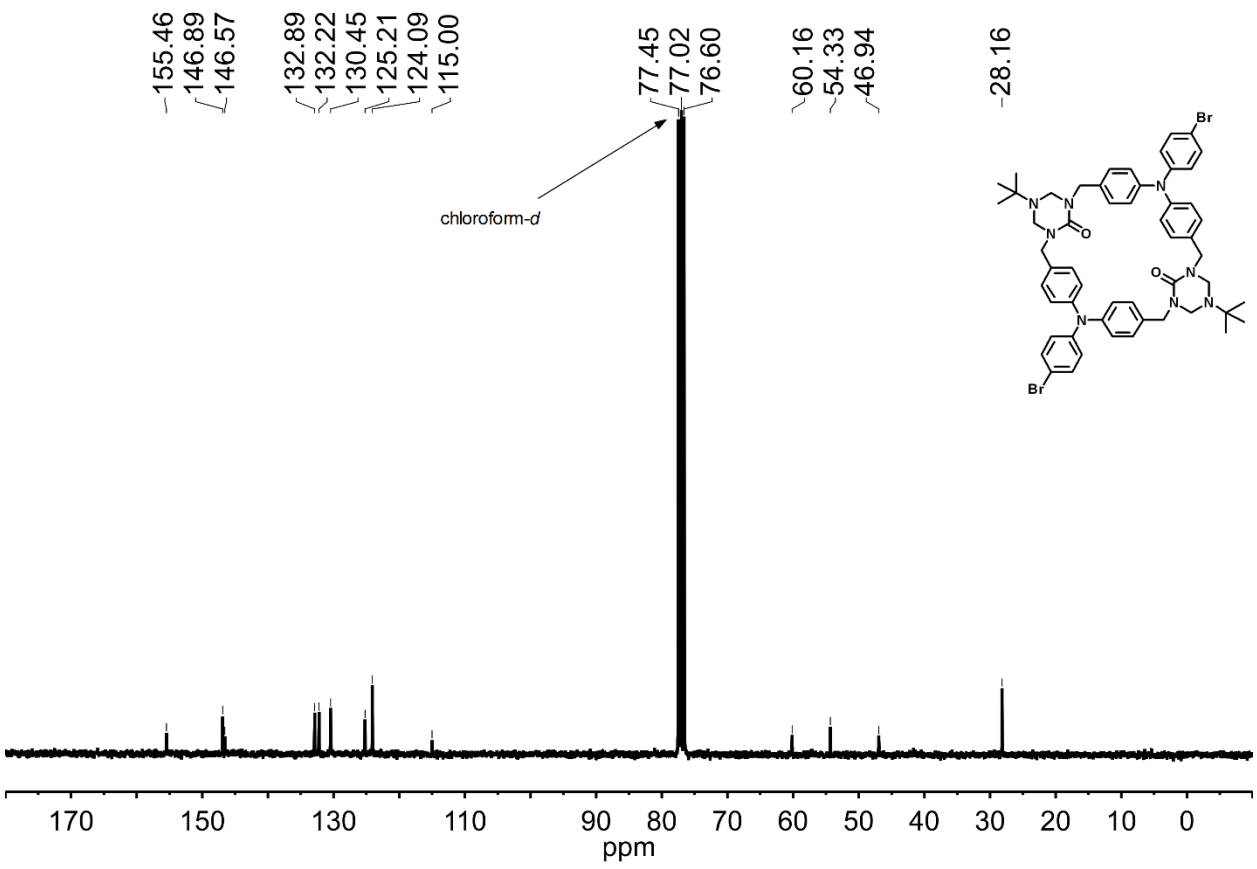

Figure S6. ^{13}C NMR ($CDCl_3$, 75 MHz)

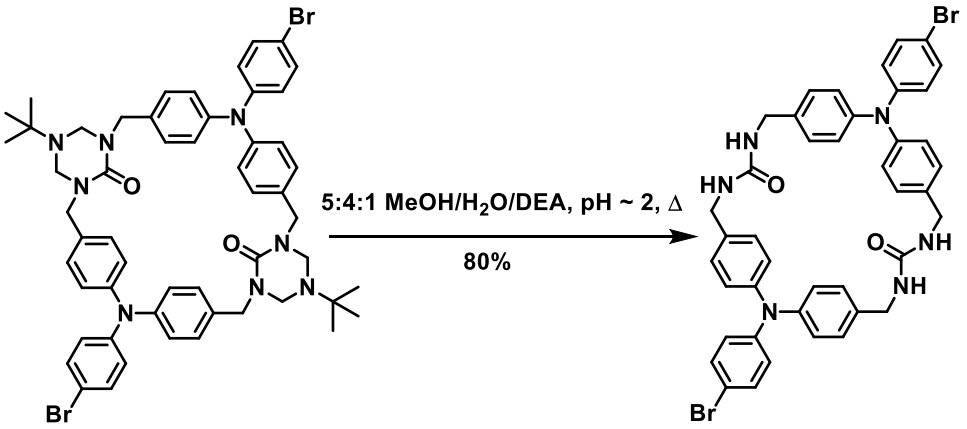

2,10-*bis*(4-Bromophenyl)-2,5,7,10,13,15-hexaaza-1,3,9,11(1,4)-tetrabenzenacyclohexadecaphane-6,14-dione: The previous protected urea (0.240 g, 0.2 mmol) was suspended in 225 mL of a 5:4:1 solution of methanol, water, and diethanol amine and the pH was adjusted to 2 using 12 M HCl. This mixture was heated at reflux for one week in the dark. During this time the pH was recalibrated to 2 every 12 hours. After cooling to room temperature, the reaction was filtered and the residue was washed with 100 mL of 1 N $HCl_{(aq)}$ then 100 mL water leaving behind the product as a beige solid (80%).^{1}H NMR (300 MHz, $(CD_3)_2SO$): δ (ppm) 7.39 (d, *J* = 8.8 Hz, 4H), 7.15 (d, *J* = 8.3 Hz, 8H), 6.93 (d, *J* = 8.3 Hz, 8H), 6.82 (d, *J* = 8.7 Hz, 4H), 6.52 (t, *J* = 6.0 Hz, 4H), 4.18 (d, *J* = 6.0 Hz, 8H). ^{13}C NMR (75 MHz, $(CD_3)_2SO$): δ (ppm) 157.80, 146.93, 145.23, 136.61, 132.07, 128.12, 124.28, 124.02, 113.40, 42.08.

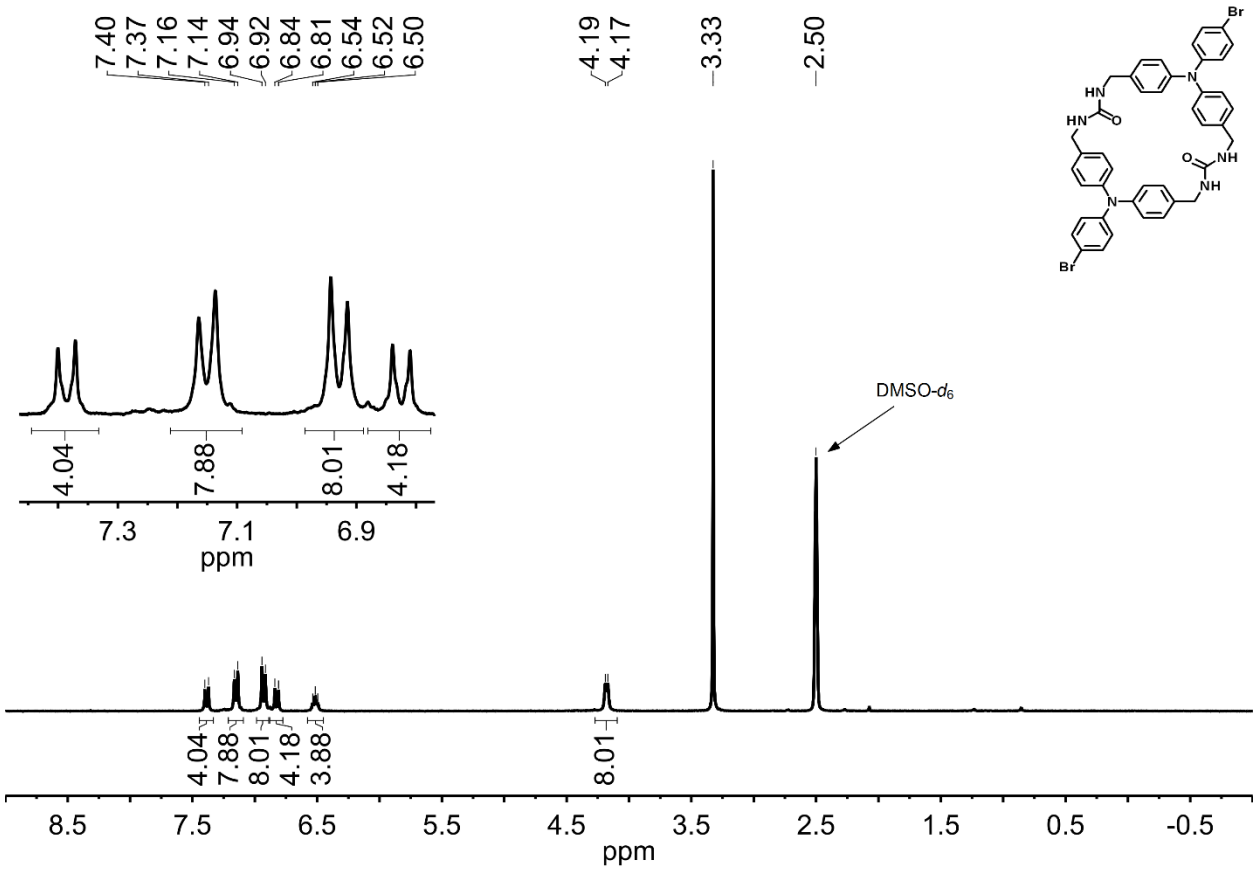

Figure S7. ^{1}H NMR ($(CD_3)_2SO$, 300 MHz)

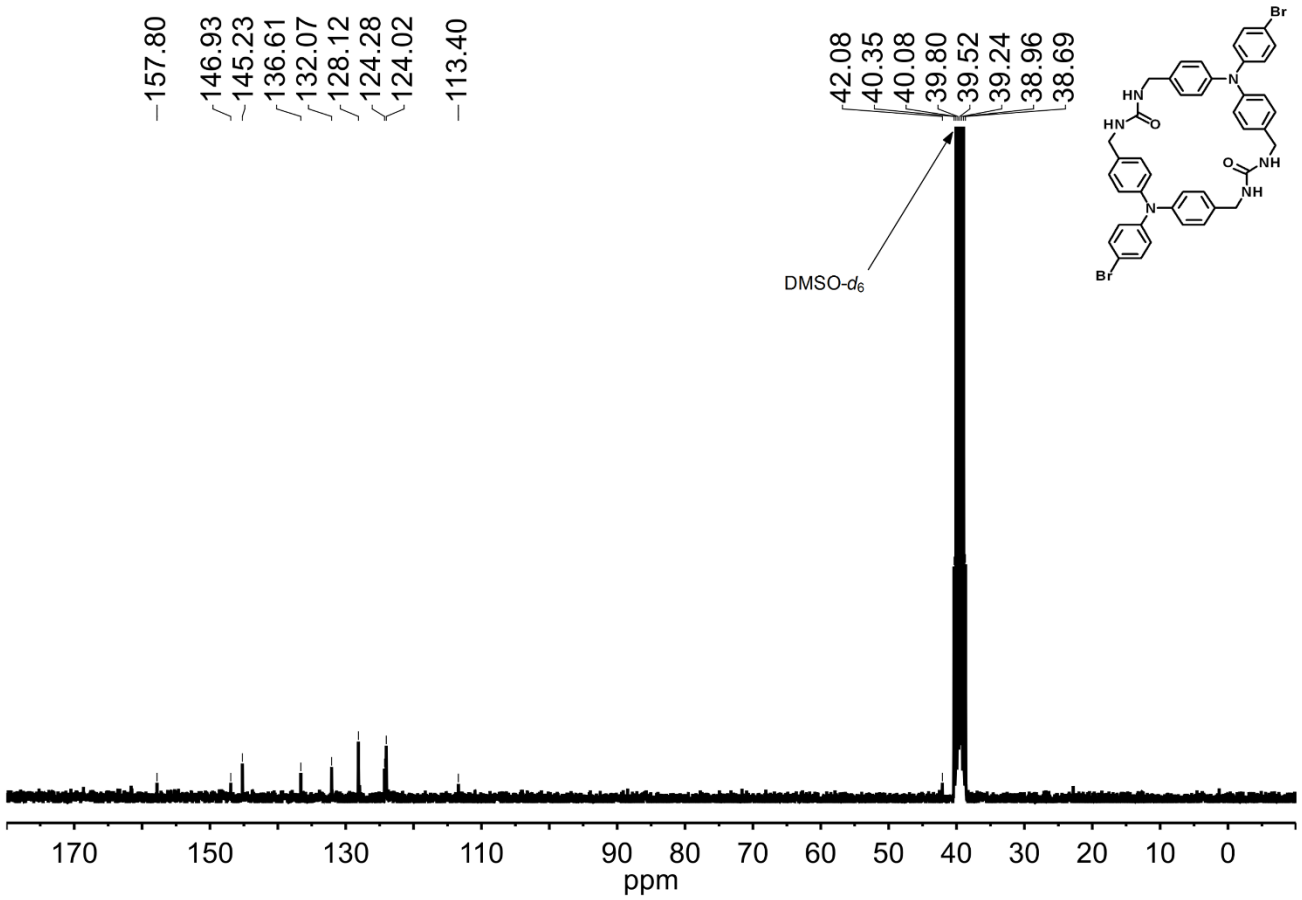

Figure S8. ^{13}C NMR ($(CD_3)_2SO$, 75 MHz)

Table S1. Data Collection and Refinement for Non-Benzene Related Crystals

Identification Code	(Protected 1)·$(CHCl_3)_8$	1·$(DME)_{0.5}$	1
CCDC	1899526	1899527	1899528
Empirical formula	$C_{62}H_{66}Br_2Cl_{24}N_8O_2$	$C_{44}H_{41}Br_2N_6O_3$	$C_{42}H_{36}Br_2N_6O_2$
Formula weight	1965.84	861.65	816.59
Temperature/K	173(2)	100(2)	100(2)
Crystal system	triclinic	monoclinic	monoclinic
Space group	P-1	$P2_1/c$	$P2_1/c$
a/Å	12.3182(5)	15.8633(11)	15.8204(7)
b/Å	12.4639(5)	4.6200(4)	4.6117(2)
c/Å	14.2206(5)	26.788(2)	26.8694(12)
α/deg	91.288(2)	90	90
β/deg	105.248(2)	100.128(2)	100.316(2)
γ/deg	95.864(2)	90	90
Volume/$Å^3$	2092.67(14)	1932.6(3)	1928.67(15)
Z	1	2	2
$\rho_{calc}g/cm^3$	1.560	1.481	1.406
μ/mm^{-1}	1.780	2.147	2.145
F(000)	988.0	882.0	832.0
Crystal size/mm^3	0.48 × 0.35 × 0.24	0.6 × 0.08 × 0.04	0.4 × 0.04 × 0.03
Radiation	MoKα (λ = 0.71073)	MoKα (λ = 0.71073)	MoKα (λ = 0.71073)
2Θ range for data collection/deg	4.318 to 50.05	4.38 to 50.164	5.234 to 55.178
Index ranges	-14 ≤ h ≤ 14, -14 ≤ k ≤ 14, -16 ≤ l ≤ 16	-18 ≤ h ≤ 18, -5 ≤ k ≤ 5, -30 ≤ l ≤ 31	-20 ≤ h ≤ 20, -6 ≤ k ≤ 6, -34 ≤ l ≤ 33
Reflections collected	66320	16686	28652
Independent reflections	7388 [R_{int} = 0.0348, R_{sigma} = 0.0204]	3424 [R_{int} = 0.0613, R_{sigma} = 0.0489]	4436 [R_{int} = 0.0610, R_{sigma} = 0.0358]
Data/restraints/parameters	7388/146/634	3424/16/269	4436/2/242
Goodness-of-fit on F^2	1.034	1.065	1.038
Final R indexes [I ≥ 2σ (I)]	R_1 = 0.0624, wR_2 = 0.1705	R_1 = 0.0403, wR_2 = 0.0920	R_1 = 0.0310, wR_2 = 0.0729
Final R indexes [all data]	R_1 = 0.0799, wR_2 = 0.1859	R_1 = 0.0605, wR_2 = 0.1001	R_1 = 0.0426, wR_2 = 0.0775
Largest diff. peak/hole / e $Å^{-3}$	0.95/-1.09	0.59/-0.55	0.51/-0.47

Table S2. Data Collection and Refinement for Benzene Derivative Loaded Host Crystals

Identification Code	$1\cdot(C_6H_6)_{0.56}$	$1\cdot(C_6H_5F)_{0.52}$	$1\cdot(C_6H_5Cl)_{0.52}$	$1\cdot(C_6H_5Br)_{0.52}$	$1\cdot(C_6H_5I)_{0.49}$
CCDC	1899529	1899530	1899531	1899532	1899533
Empirical formula	$C_{45.38}H_{39.38}Br_2N_6O_2$	$C_{45}H_{38.5}Br_2F_{0.5}N_6O_2$	$C_{45.14}H_{38.62}Br_2Cl_{0.52}N_6O_2$	$C_{45.09}H_{38.58}Br_{2.52}N_6O_2$	$C_{44.98}H_{38.48}Br_2I_{0.5}N_6O_2$
Formula weight	860.52	864.64	875.54	897.51	917.63
Temperature/K	100(2)	100(2)	100(2)	100(2)	100(2)
Crystal system	monoclinic	monoclinic	monoclinic	monoclinic	monoclinic
Space group	$P2_1/c$	$P2_1/c$	$P2_1/c$	$P2_1/c$	$P2_1/c$
a/Å	15.8777(5)	15.8857(6)	15.8533(6)	15.8509(6)	15.8680(5)
b/Å	4.6345(2)	4.6310(2)	4.6332(2)	4.6392(2)	4.6477(2)
c/Å	26.7173(8)	26.7350(10)	26.7661(10)	26.7433(9)	26.6829(9)
α/deg	90	90	90	90	90
β/deg	99.975(2)	99.910(2)	100.069(2)	100.019(2)	100.071(2)
γ/deg	90	90	90	90	90
Volume/$Å^3$	1936.28(12)	1937.46(13)	1935.73(13)	1936.59(13)	1937.53(12)
Z	2	2	2	2	2
$\rho_{calc}g/cm^3$	1.476	1.482	1.502	1.539	1.573
μ/mm^{-1}	2.141	2.142	2.178	2.672	2.534
F(000)	879.0	882.0	893.0	910.0	925.0
Crystal size/mm^3	0.28 × 0.04 × 0.03	0.14 × 0.06 × 0.03	0.1 × 0.06 × 0.02	0.12 × 0.04 × 0.03	0.22 × 0.05 × 0.03
Radiation	MoKα (λ = 0.71073)	MoKα (λ = 0.71073)	MoKα (λ = 0.71073)	MoKα (λ = 0.71073)	MoKα (λ = 0.71073)
2Θ range for data collection/deg	3.684 to 50.148	4.372 to 50.098	3.68 to 50.104	2.61 to 48.61	2.606 to 52.768
Index ranges	-18 ≤ h ≤ 18, -4 ≤ k ≤ 5, -31 ≤ l ≤ 31	-18 ≤ h ≤ 18, -5 ≤ k ≤ 5, -31 ≤ l ≤ 31	-18 ≤ h ≤ 18, -5 ≤ k ≤ 5, -31 ≤ l ≤ 31	-18 ≤ h ≤ 18, -4 ≤ k ≤ 5, -30 ≤ l ≤ 30	-19 ≤ h ≤ 19, -5 ≤ k ≤ 5, -33 ≤ l ≤ 33
Reflections collected	22892	19628	18624	16210	37894
Independent reflections	3428 [R_{int} = 0.0644, R_{sigma} = 0.0354]	3422 [R_{int} = 0.0611, R_{sigma} = 0.0369]	3419 [R_{int} = 0.0665, R_{sigma} = 0.0414]	3149 [R_{int} = 0.0861, R_{sigma} = 0.0548]	3962 [R_{int} = 0.0607, R_{sigma} = 0.0270]
Data/restraints/parameters	3428/21/281	3422/4/259	3419/7/274	3149/6/276	3962/90/281
Goodness-of-fit on F^2	1.067	1.058	1.063	1.032	1.050
Final R indexes [I ≥ 2σ (I)]	R_1 = 0.0395, wR_2 = 0.0882	R_1 = 0.0461, wR_2 = 0.1076	R_1 = 0.0417, wR_2 = 0.0905	R_1 = 0.0452, wR_2 = 0.0971	R_1 = 0.0369, wR_2 = 0.0840
Final R indexes [all data]	R_1 = 0.0547, wR_2 = 0.0944	R_1 = 0.0651, wR_2 = 0.1163	R_1 = 0.0597, wR_2 = 0.0982	R_1 = 0.0729, wR_2 = 0.1081	R_1 = 0.0473, wR_2 = 0.0889
Largest diff. peak/hole / e $Å^{-3}$	0.59/-0.44	1.09/-0.65	0.67/-0.44	0.66/-0.42	0.67/-0.46

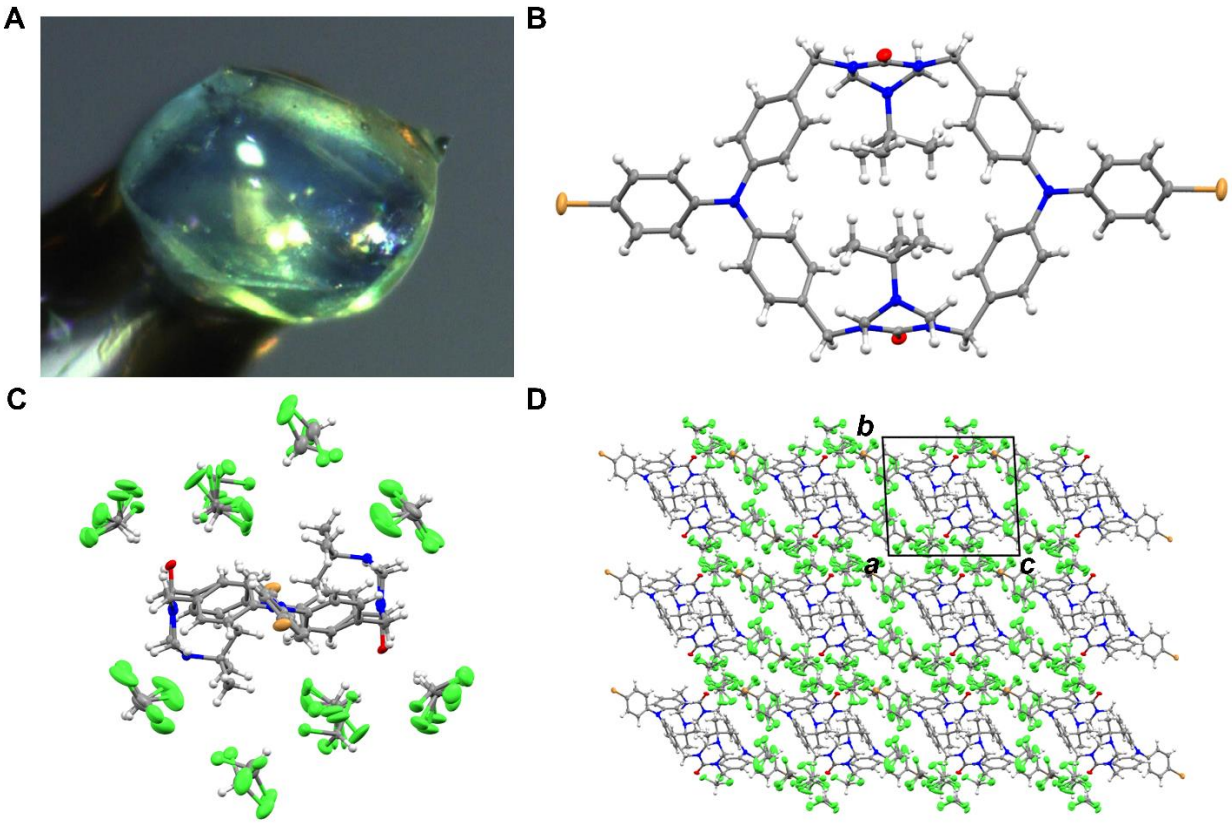

Figure S9. Crystal views of (Protected **1**)·$(CHCl_3)_8$. (A) Data crystal coated with oil and mounted on the diffractometer at T = 173(2) K. (B) Molecular structure of protected **1**, (C) one unit cell, and (D) crystal packing along the *a* axis. Thermal ellipsoids were drawn at the 30% probability level.

Crystals formed as visually perfect colorless blocks. They are extremely unstable with respect to solvent loss and crumble to a powder within seconds of removal from the mother liquor. If transferred rapidly from the mother liquor into a drop of oil (*e.g* paratone-N), they can be handled for minutes before decomposition. They were also observed to fracture and suffer degraded crystallinity when flash-cooled at temperatures below *ca*. 150 K. X-ray intensity data were collected at 173(2) K using a Bruker D8 QUEST diffractometer equipped with a PHOTON-100 CMOS area detector and an Incoatec microfocus source (Mo Kα radiation, λ = 0.71073 Å). The raw area detector data frames were reduced and corrected for absorption effects using the Bruker APEX3, SAINT+ and SADABS programs.[2,3] Final unit cell parameters were determined by least-squares refinement of 9408 reflections taken from the data set. The structure

was solved with SHELXT.[4,5] Subsequent difference Fourier calculations and full-matrix least-squares refinement against F^2 were performed with SHELXL-2018[4,5] using OLEX2.[6]

The compound crystallizes in the triclinic system. The space group *P*-1 (No. 2) was confirmed by structure solution. The asymmetric unit consists of half of one $C_{54}H_{58}Br_2N_8O_2$ molecule, which is located on a crystallographic inversion center, and four independent chloroform molecules. All four $CHCl_3$ molecules are disordered and were modeled with two, three or four components. The total site occupancy for each molecule was constrained to sum to one. C-Cl distances were restrained to 1.75(2) Å, and all Cl-Cl distances were restrained to be similar. All non-hydrogen atoms were refined with anisotropic displacement parameters. Anisotropic displacement parameters for nearly overlapped atoms of the disordered chloroform molecules were held equal. Hydrogen were placed in geometrically idealized positions and included as riding atoms with *d*(C-H) = 1.00 Å and *U*iso(H) = 1.2*U*eq(C) for methine hydrogen atoms, *d*(C-H) = 0.95 Å and *U*iso(H) = 1.2*U*eq(C) for aromatic hydrogen atoms, *d*(C-H) = 0.99 Å and *U*iso(H) = 1.2*U*eq(C) for methylene hydrogen atoms, and *d*(C-H) = 0.98 Å and *U*iso(H) = 1.5*U*eq(C) for methyl hydrogens. The methyl hydrogens were allowed to rotate as a rigid group to the orientation of maximum observed electron density. The largest residual electron density peak in the final difference map is 0.95 $e^-/Å^3$, located 1.95 Å from Cl29.

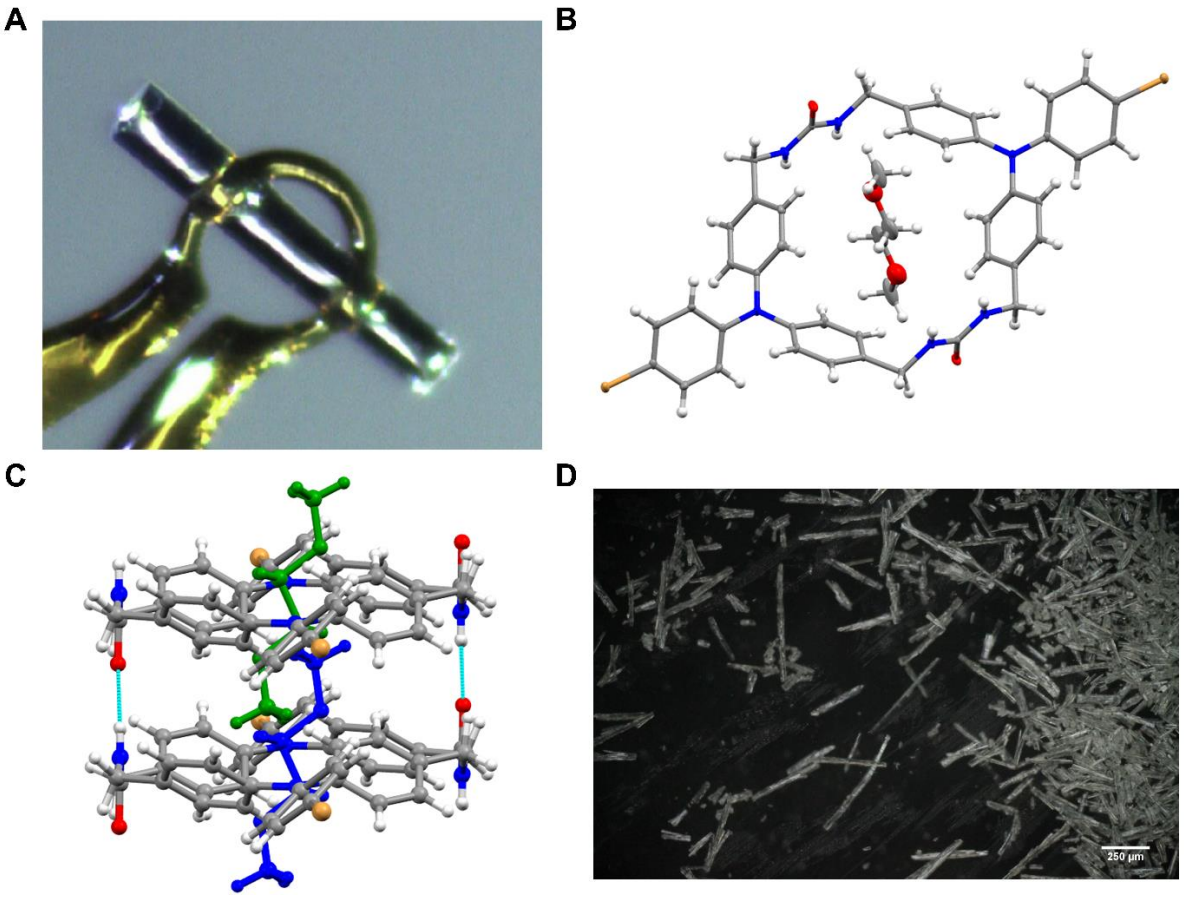

Figure S10. Crystal views of **1**·$(DME)_{0.5}$. (A) Data crystal. (B) Components of structure. Thermal ellipsoids were drawn at the 30% probability level. (C) View of DME disorder inside the host **1**. (D) Picture of crystals using an Olympus BX-51 epifluorescence microscope using a 5× objective lens in dark field mode. Image was collected with a color digital CMOS camera (Canon EOS REBEL T3/1100D). Scale bar is set at 250 µm. An average crystal size of 35 x 265 µm was found by measuring multiple crystals.

X-ray intensity data from a colorless needle were collected at 100(2) K using a Bruker D8 QUEST diffractometer equipped with a PHOTON-100 CMOS area detector and an Incoatec microfocus source (Mo Kα radiation, λ = 0.71073 Å). The raw area detector data frames were reduced and corrected for absorption effects with the Bruker APEX3, SAINT+ and SADABS programs.[2,3] The structure was solved with

SHELXT.[4,5] Subsequent difference Fourier calculations and full-matrix least-squares refinement against F^2 were performed with SHELXL-2018[4,5] using OLEX2.[6]

The compound crystallizes in the monoclinic system. The pattern of systematic absences in the intensity data was uniquely consistent with the space group $P2_1/c$, which was confirmed by structure solution. The asymmetric unit consists of half of one $C_{42}H_{36}Br_2N_6O_2$ cycle and (formally) ¼ of one glyme (1,2-dimethoxyethane) molecule. The glyme molecule is located on a crystallographic inversion center and is further disordered over another inversion center. The three symmetry-independent atoms of this molecule were refined with fixed occupancies of 0.5. Appropriate C-C and C-O distance restraints were applied. All non-hydrogen atoms were refined with anisotropic displacement parameters. Enhanced rigid-bond restraints (SHELX RIGU) was applied to the U_{ij} coefficients of the disordered glyme atom displacement parameters. Hydrogen atoms bonded to carbon were placed in geometrically idealized positions and included as riding atoms with *d*(C-H) = 0.95 Å and *U*iso(H) = 1.2*U*eq(C) for aromatic hydrogen atoms, *d*(C-H) = 0.99 Å and *U*iso(H) = 1.2*U*eq(C) for methylene hydrogen atoms, and *d*(C-H) = 0.98 Å and *U*iso(H) = 1.5*U*eq(C) for methyl hydrogens. The methyl hydrogens were allowed to rotate as a rigid group to the orientation of maximum observed electron density. N-H hydrogen atoms were located in a difference maps and refined with *d*(N-H) = 0.84(2) Å distance restraints and *U*iso(H) = 1.2*U*eq(N). The largest residual electron density peak in the final difference map is 0.59 $e^-/Å^3$, located 0.34 Å from H1SA.

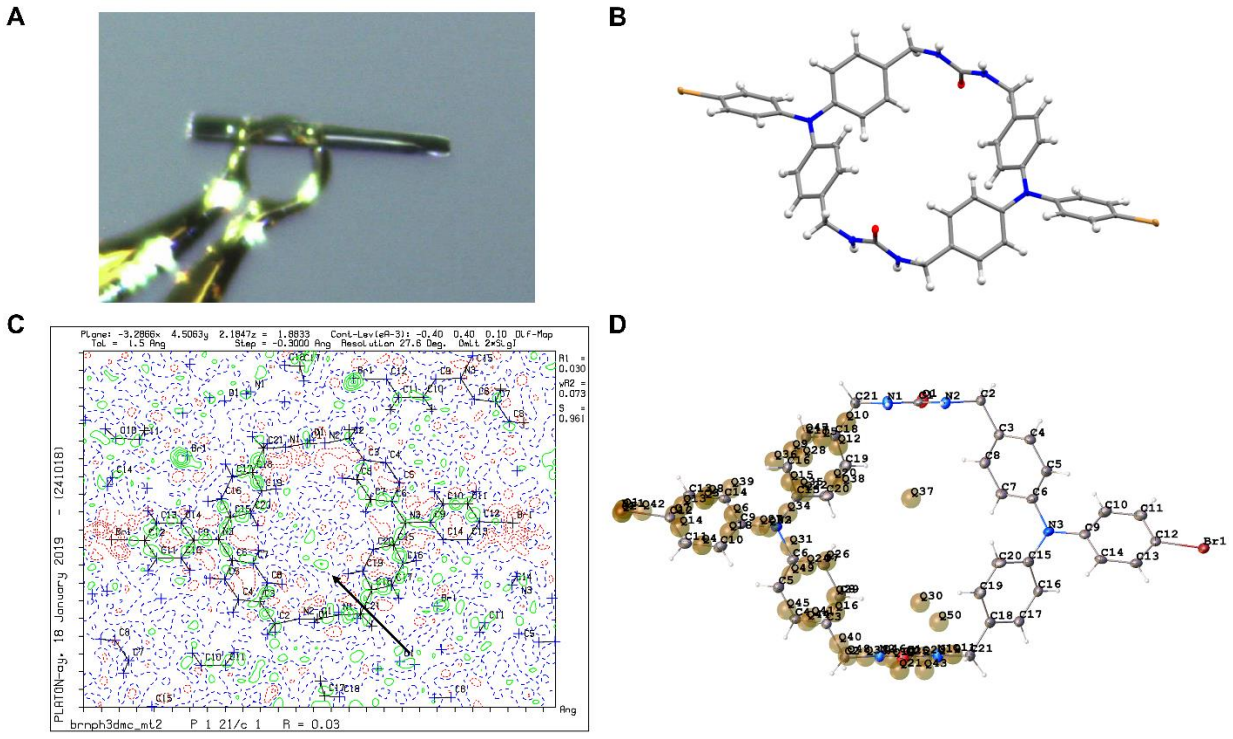

Figure S11. Crystal views of **1**. (A) Data crystal for second data set. (B) Molecular structure. Thermal ellipsoids were drawn at the 30% probability level. (C) Difference electron density contour map. Solid green contours represent positive electron density, red dashed lines negative electron density, and blue dashed lines zero e-/Å^3 contours. The maximum observed electron density of 0.19 e-/Å^3 inside the cycle column is marked with an arrow. (D) Difference electron density shown as SHELXL "Q-peaks". Q30 has magnitude of 0.20 e-/Å^3; Q37 is 0.19 e-/Å^3.

X-ray intensity data from colorless needles were collected at 100(2) K using a Bruker D8 QUEST diffractometer equipped with a PHOTON-100 CMOS area detector and an Incoatec microfocus source (Mo Kα radiation, λ = 0.71073 Å). The raw area detector data frames were reduced and corrected for absorption effects using the Bruker APEX3, SAINT+ and SADABS programs.[2,3] The structure was solved with SHELXT.[4,5] Subsequent difference Fourier calculations and full-matrix least-squares refinement against F^2 were performed with SHELXL-2018[4,5] using OLEX2.[6]

The compound crystallizes in the monoclinic system. The pattern of systematic absences in the intensity data was consistent with the space group $P2_1/c$, which was confirmed by structure solution. The asymmetric unit consists of half of one $C_{42}H_{36}Br_2N_6O_2$ molecule, which is located on a crystallographic inversion center. All non-hydrogen atoms were refined with anisotropic displacement parameters. Hydrogen atoms bonded to carbon were located in difference Fourier maps before being placed in geometrically idealized positions and included as riding atoms with *d*(C-H) = 0.95 Å and *U*iso(H) = 1.2*U*eq(C) for aromatic hydrogen atoms and *d*(C-H) = 0.99 Å and *U*iso(H) = 1.2*U*eq(C) for methylene hydrogen atoms. Hydrogen atoms bonded to the urea nitrogen atoms were located and refined with a common isotropic displacement parameter and *d*(N-H) = 0.85(2) Å. The largest residual electron density peak and hole in the final difference map are +0.50 $e^-/Å^3$ and -0.47 $e^-/Å^3$, located 1.02 Å and 0.91 Å from Br1, respectively.

The difference electron density map was inspected carefully for residual electron density in the interior of the columns formed by the $C_{42}H_{36}Br_2N_6O_2$ cycle, where solvent molecules were located before heating. Datasets were collected from two separate single crystals. The first dataset (crystal 1) came from a specimen selected immediately after removing the sample from the heating apparatus (TGA) used to remove the solvent guests. The second dataset (crystal 2) was from a crystal which had been exposed to air for three days. The results from the two datasets were essentially identical. No significant electron density was observed in interior of the columns formed by the cycles. The largest residual peaks inside the columns had magnitudes of 0.21 e-/$Å^3$ (crystal no. 1, Q-peak #40 in the SHELXL list) and 0.19 $e^-/Å^3$ (crystal no. 2, SHELXL Q-peak #37). Trial refinements of this peak as a partially occupied carbon atom resulted in an occupancy value of 0.03(2), within experimental error of zero (crystal 1). No change in *R*-values or difference map features was observed upon including this peak in the refinement. It is concluded then, that the peak is simply background noise and does not arise from atomic electron density, and

further, that the column interior is effectively empty to within the detection limit of the single crystal X-ray diffraction technique.

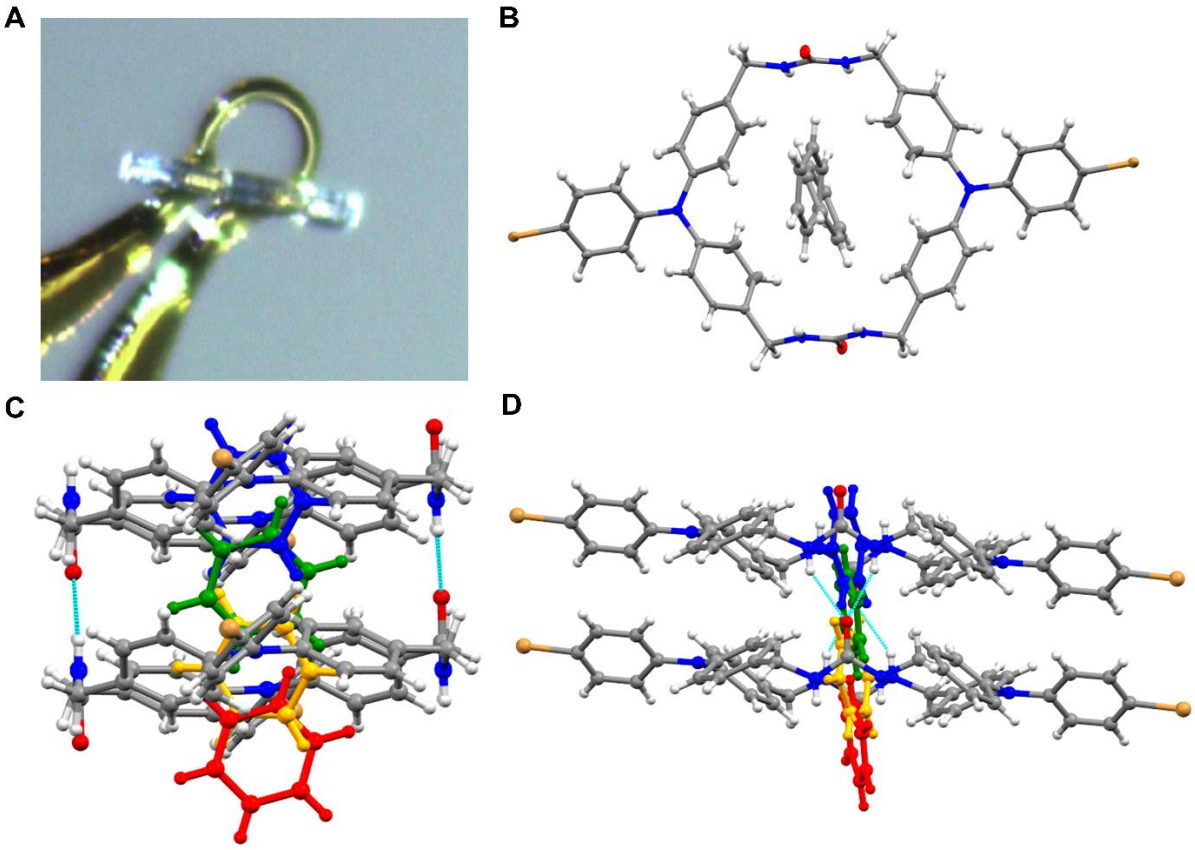

Figure S12. Crystal views of **1**·$(C_6H_6)_{0.56}$. (A) Data crystal. (B) Components of structure. Thermal ellipsoids were drawn at the 30% probability level. (C) View of C_6H_6 disorder inside the host **1**. (D) Another view of the disorder.

X-ray intensity data from a colorless needle were collected at 100(2) K using a Bruker D8 QUEST diffractometer equipped with a PHOTON-100 CMOS area detector and an Incoatec microfocus source (Mo Kα radiation, λ = 0.71073 Å). The raw area detector data frames were reduced and corrected for absorption effects using the Bruker APEX3, SAINT+ and SADABS programs.[2,3] The structure was solved with SHELXT.[4,5] Subsequent difference Fourier calculations and full-matrix least-squares refinement against F^2 were performed with SHELXL-2018[4,5] using OLEX2.[6]

The compound crystallizes in the space group $P2_1/c$ of the monoclinic system. The asymmetric unit consists of half of one $C_{42}H_{36}Br_2N_6O_2$ cycle located on a crystallographic inversion center and several

electron density peaks inside the tubular channels created by the cycle columns. The residual difference electron density in the channel region is disordered, but arranged in a tapelike fashion along the crystallographic *b* axis direction. If assigned as carbon atoms, all peaks refined to less than full occupancy. The peaks could be reasonably fitted to half each (3 carbon atoms) of two crystallographically independent benzene molecules, both located on crystallographic inversion centers. All 1,2-C-C distances in the benzene guests were restrained to *d* = 1.40(2) Å. 1,4-C-C (opposite) distances were restrained to be similar to each other (SHELX SADI), and the minor component (C4S-C6S) was further restrained to be flat (SHELX FLAT). Occupancies refined to: C1S-C3S = 0.437(5) and C4S-C6S = 0.126(9), generating a C_6H_6 composition per cycle of 0.56(1). The benzene group occupancies were linked so that the sum of occupancies of benzene molecules within van der Waals radii of other benzenes was not greater than one. All non-hydrogen atoms were refined with anisotropic displacement parameters, except for atoms of the minor benzene component, which were assigned a common isotropic displacement parameter. Hydrogen atoms bonded to carbon were placed in geometrically idealized positions and included as riding atoms with *d*(C-H) = 0.95 Å and *U*iso(H) = 1.2*U*eq(C) for aromatic hydrogen atoms and *d*(C-H) = 0.99 Å and *U*iso(H) = 1.2*U*eq(C) for methylene hydrogen atoms. The two urea hydrogen atoms were located and refined with *d*(N-H) = 0.85(2) Å distance restraints and *U*iso(H) = 1.2*U*eq(N). The largest residual electron density peak in the final difference map is 0.59 $e^-/Å^3$, located 1.08 Å from Br1.

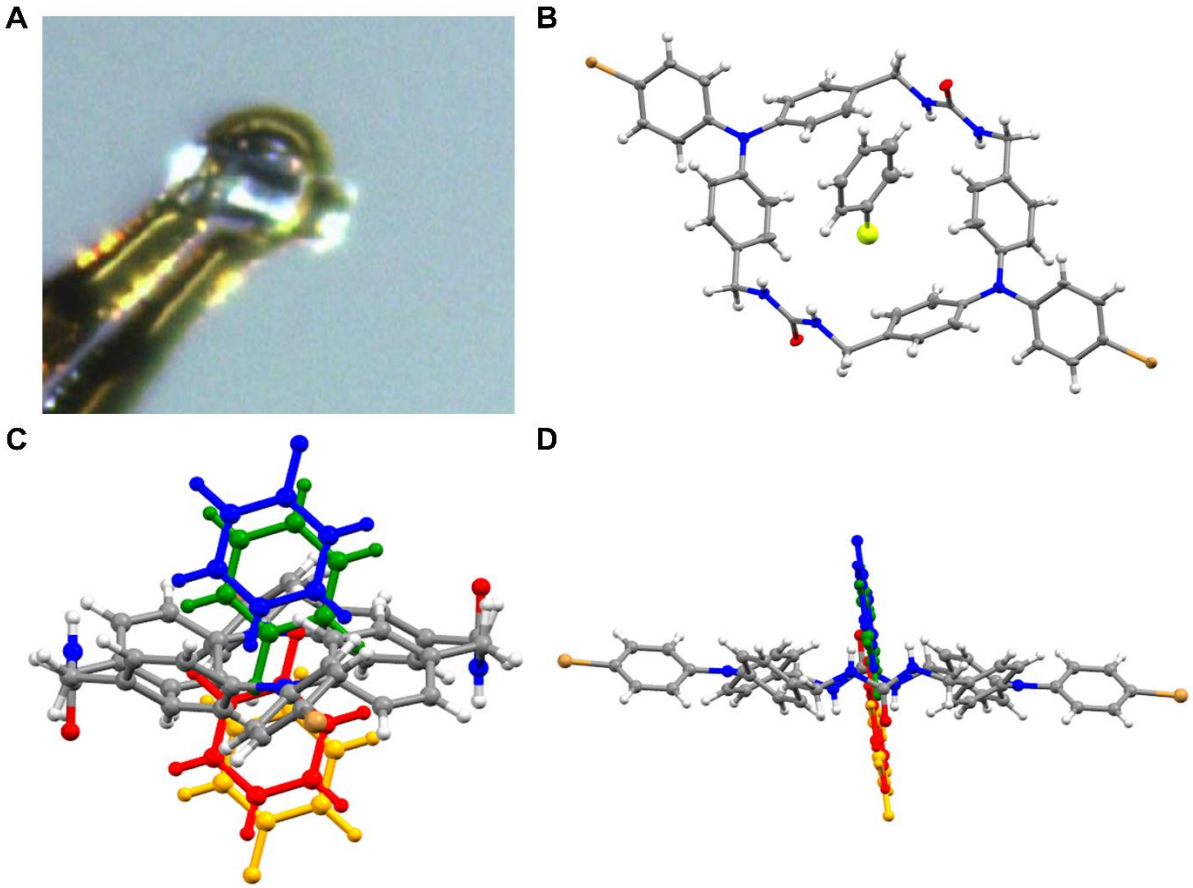

Figure S13. Crystal views of **1**·$(C_6H_5F)_{0.52}$. (A) Data crystal. (B) Components of structure. Thermal ellipsoids were drawn at the 30% probability level. (C) View of C_6H_5F disorder inside the host **1**. (D) Another view of the disorder.

X-ray intensity data from a colorless needle were collected at 100(2) K using a Bruker D8 QUEST diffractometer equipped with a PHOTON-100 CMOS area detector and an Incoatec microfocus source (Mo Kα radiation, λ = 0.71073 Å). The raw area detector data frames were reduced and corrected for absorption effects using the Bruker APEX3, SAINT+ and SADABS programs.[2,3] The structure was solved with SHELXT.[4,5] Subsequent difference Fourier calculations and full-matrix least-squares refinement against F^2 were performed with SHELXL-2018[4,5] using OLEX2.[6]

The compound crystallizes in the space group $P2_1/c$ of the monoclinic system. The asymmetric unit consists of half of one $C_{42}H_{36}Br_2N_6O_2$ cycle located on a crystallographic inversion center and disordered fluorobenzene molecules located in channels created by the cycle packing. The fluorobenzene molecules are disordered within planar 'tapes' running along the crystallographic *b* axis direction. One crystallographically independent C_6H_5F was modeled, which is disordered over two sites about a crystallographic inversion center. Translational symmetry brings two additional symmetry-related C_6H_5F molecules in close proximity, and therefore the maximum crystallographic occupancy for each C_6H_5F disorder component is 0.25. Free refinement of the C_6H_5F occupancy yielded 0.26(1), but was fixed at 0.25 for the final model. The phenyl rings was fitted to a regular hexagonal with *d*(C-C) = 1.39 Å, and appropriate C-F distance restraints were applied. All non-hydrogen atoms were refined with anisotropic displacement parameters except for disordered fluorobenzene atoms (isotropic). Hydrogen atoms bonded to carbon were located in difference Fourier maps before being placed in geometrically idealized positions and included as riding atoms with *d*(C-H) = 0.95 Å and *U*iso(H) = 1.2*U*eq(C) for aromatic hydrogen atoms and *d*(C-H) = 0.99 Å and *U*iso(H) = 1.2*U*eq(C) for methylene hydrogen atoms. The two urea hydrogen atoms were located in difference Fourier maps and refined isotropically with *d*(N-H) = 0.84(2) distance restraints. The largest residual electron density peak in the final difference map is 1.09 $e^-/Å^3$, located 1.11 Å from C3S.

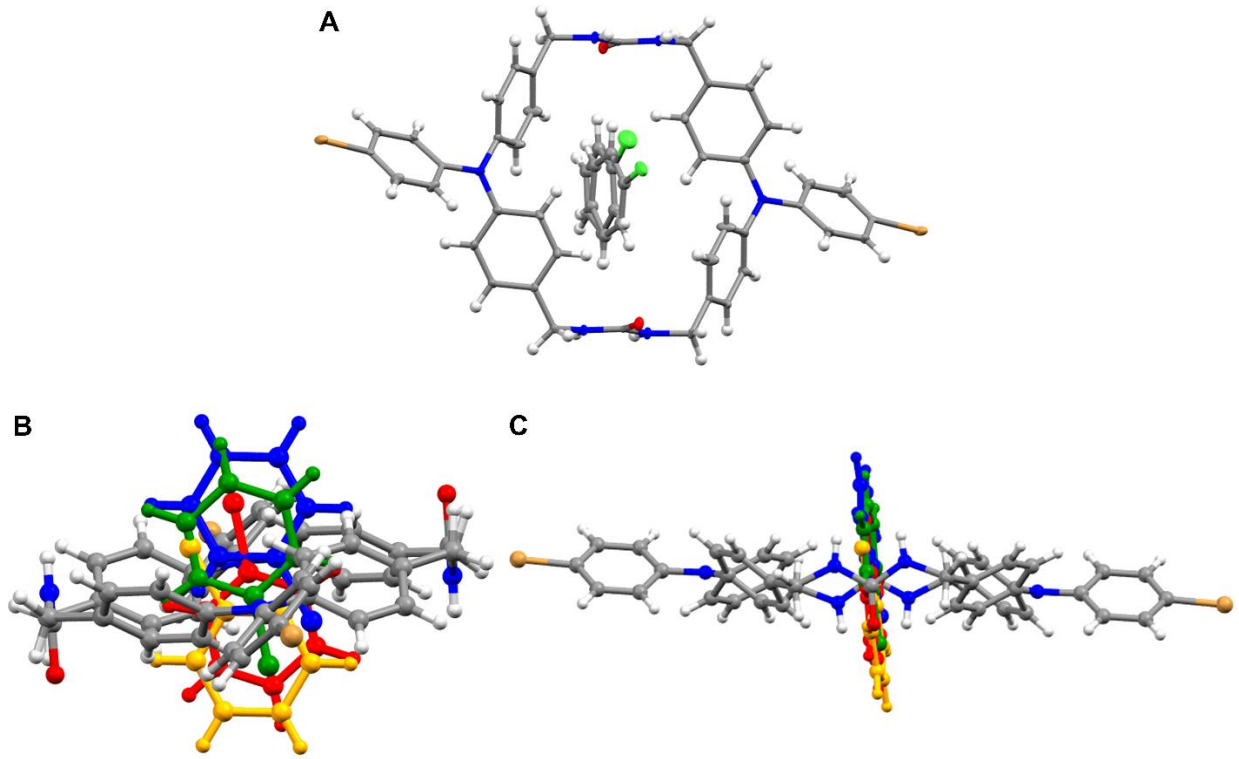

Figure S14. Crystal views of **1**·$(C_6H_5Cl)_{0.52}$. (A) Data crystal. (B) Components of structure. Thermal ellipsoids were drawn at the 30% probability level. (C) View of C_6H_5Cl disorder inside the host **1**. (D) Another view of the disorder.

X-ray intensity data from a colorless needle were collected at 100(2) K using a Bruker D8 QUEST diffractometer equipped with a PHOTON-100 CMOS area detector and an Incoatec microfocus source (Mo Kα radiation, λ = 0.71073 Å). The raw area detector data frames were reduced and corrected for absorption effects using the Bruker APEX3, SAINT+ and SADABS programs.[2,3] The structure was solved with SHELXT.[4,5] Subsequent difference Fourier calculations and full-matrix least-squares refinement against F^2 were performed with SHELXL-2018[4,5] using OLEX2.[6]

The compound crystallizes in the space group $P2_1/c$ of the monoclinic system. The asymmetric unit consists of half of one $C_{42}H_{36}Br_2N_6O_2$ cycle located on a crystallographic inversion center and several electron density peaks inside the tubular channels created by the cycle columns. The residual difference electron density in the channel region is highly disordered, but arranged in a tapelike planar fashion along

the crystallographic *b* axis direction. If assigned as carbon atoms, most peaks refined to less than full occupancy. Two peaks refined to significantly greater than or near 100% carbon occupancy. These were assumed to be chlorine atoms from the crystal soaking agent chlorobenzene. Two independent, partially occupied C_6H_5Cl molecules were modeled. Both are further disordered about a crystallographic inversion center. The phenyl rings of each were fitted to rigid hexagons, and both bonded C-Cl distances were restrained to 1.74(2) Å. 1,3-C-Cl distances were restrained to be similar to each other (SHELX SADI). Occupancies refined to: Cl1S/C1S-C6S = 0.187(3) and Cl2S/C7S-C12S = 0.074(3), generating a C_6H_5Cl composition per cycle of 0.523(6). All non-hydrogen atoms were refined with anisotropic displacement parameters. All carbon atoms of the chlorobenzene C_6 rings were assigned a common isotropic displacement parameter. Hydrogen atoms bonded to carbon were placed in geometrically idealized positions and included as riding atoms with *d*(C-H) = 0.95 Å and *U*iso(H) = 1.2*U*eq(C) for aromatic hydrogen atoms and *d*(C-H) = 0.99 Å and *U*iso(H) = 1.2*U*eq(C) for methylene hydrogen atoms. The two urea hydrogen atoms were located and refined with *d*(N-H) = 0.84(2) Å distance restraints and *U*iso(H) = 1.2*U*eq(N). The largest residual electron density peak in the final difference map is 0.67 $e^-/Å^3$, located 0.56 Å from C1S.

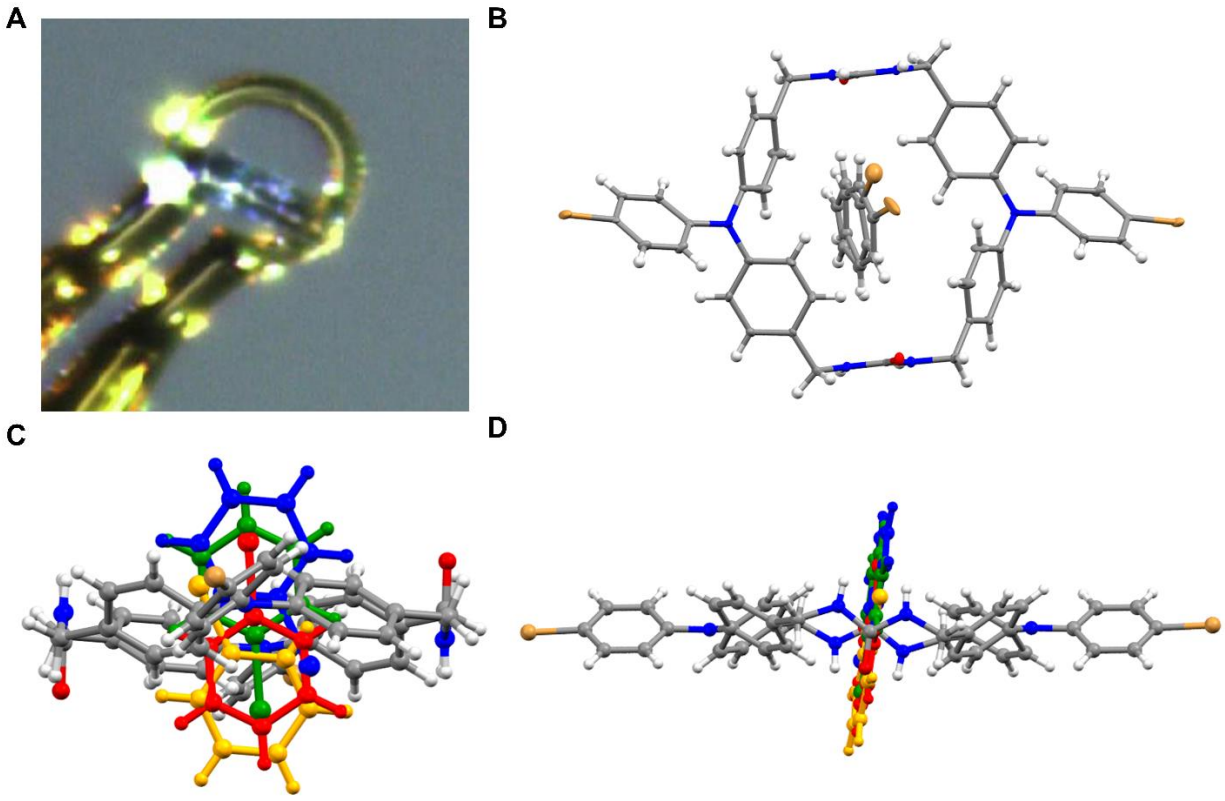

Figure S15. Crystal views of **1**·$(C_6H_5Br)_{0.52}$. (A) Data crystal. (B) Components of structure. Thermal ellipsoids were drawn at the 30% probability level. (C) View of C_6H_5Br disorder inside the host **1**. (D) Another view of the disorder.

X-ray intensity data from a colorless needle were collected at 100(2) K using a Bruker D8 QUEST diffractometer equipped with a PHOTON-100 CMOS area detector and an Incoatec microfocus source (Mo Kα radiation, λ = 0.71073 Å). The raw area detector data frames were reduced and corrected for absorption effects using the Bruker APEX3, SAINT+ and SADABS programs.[2,3] The structure was solved with SHELXT.[4,5] Subsequent difference Fourier calculations and full-matrix least-squares refinement against F^2 were performed with SHELXL-2018[4,5] using OLEX2.[6]

The compound crystallizes in the space group $P2_1/c$ of the monoclinic system. The asymmetric unit consists of half of one $C_{42}H_{36}Br_2N_6O_2$ cycle located on a crystallographic inversion center and several electron density peaks inside the tubular channels created by the cycle columns. The residual difference

electron density in the channel region is highly disordered, but arranged in a tapelike planar fashion along the crystallographic *b* axis direction. If assigned as carbon atoms, most peaks refined to less than full occupancy. Two peaks refined to significantly greater than or near 100% carbon occupancy. These were assumed to be bromine atoms from the crystal soaking agent bromobenzene. Two independent, partially occupied C_6H_5Br molecules were modeled. Both are further disordered about a crystallographic inversion center. The phenyl rings of each were fitted to rigid hexagons, and both bonded C-Br distances were restrained to 1.90(2) Å. 1,3-C-Br distances were restrained to be similar to each other (SHELX SADI). Occupancies refined to: Br1S/C1S-C6S = 0.187(2) and Br2S/C7S-C12S = 0.071(2), generating a C_6H_5Br composition per cycle of 0.516(6). All non-hydrogen atoms were refined with anisotropic displacement parameters. All carbon atoms of the bromobenzene C_6 rings were assigned a common isotropic displacement parameter. Hydrogen atoms bonded to carbon were placed in geometrically idealized positions and included as riding atoms with *d*(C-H) = 0.95 Å and *U*iso(H) = 1.2*U*eq(C) for aromatic hydrogen atoms and *d*(C-H) = 0.99 Å and *U*iso(H) = 1.2*U*eq(C) for methylene hydrogen atoms. The two urea hydrogen atoms were refined isotropically with *d*(N-H) = 0.84(2) Å distance restraints. The largest residual electron density peak in the final difference map is 0.66 $e^-/Å^3$, located 0.52 Å from H4S.

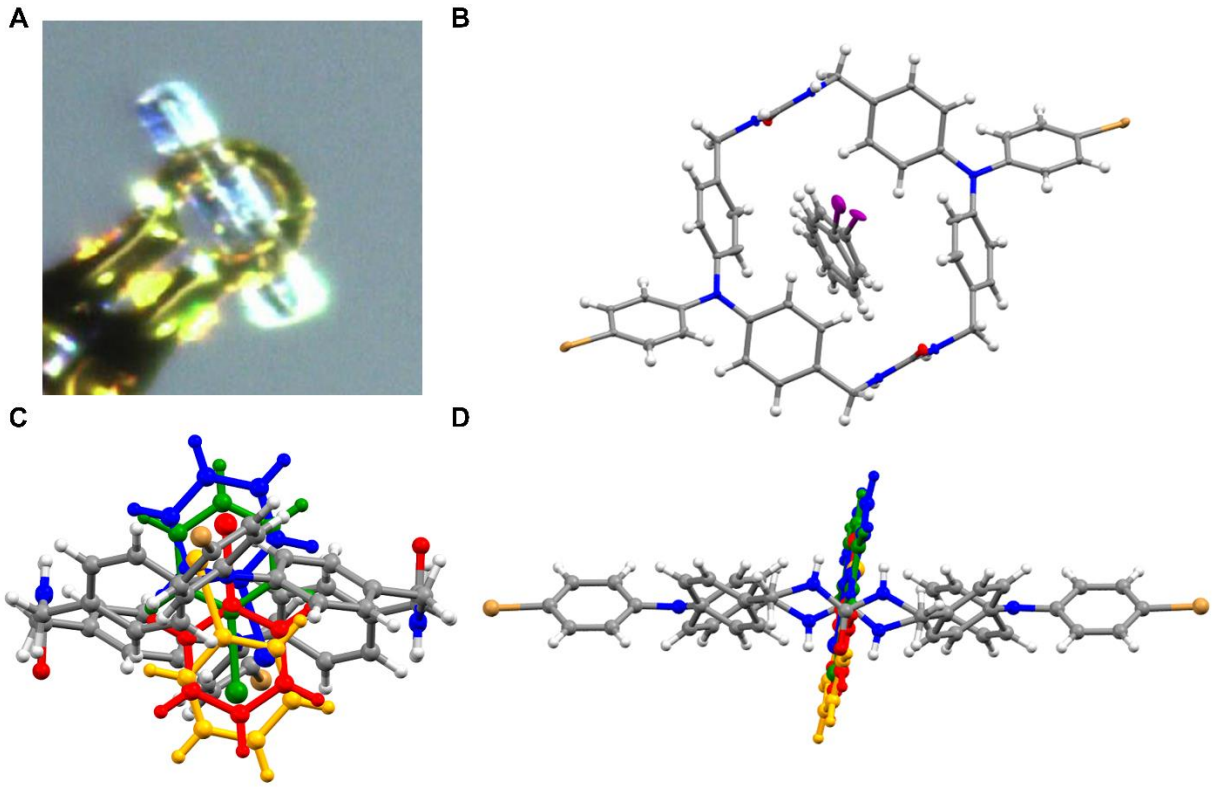

Figure S16. Crystal views of **1**·$(C_6H_5I)_{0.49}$. (A) Data crystal. (B) Components of structure. Thermal ellipsoids were drawn at the 30% probability level. (C) View of C_6H_5I disorder inside the host **1**. (D) Another view of the disorder.

X-ray intensity data from a colorless needle were collected at 100(2) K using a Bruker D8 QUEST diffractometer equipped with a PHOTON-100 CMOS area detector and an Incoatec microfocus source (Mo Kα radiation, λ = 0.71073 Å). The raw area detector data frames were reduced and corrected for absorption effects using the Bruker APEX3, SAINT+ and SADABS programs.[2,3] The structure was solved with SHELXT.[4,5] Subsequent difference Fourier calculations and full-matrix least-squares refinement against F^2 were performed with SHELXL-2018[4,5] using OLEX2.[6]

The compound crystallizes in the space group $P2_1/c$ of the monoclinic system. The asymmetric unit consists of half of one $C_{42}H_{36}Br_2N_6O_2$ cycle located on a crystallographic inversion center and several electron density peaks inside the tubular channels created by the cycle columns. The residual difference

electron density in the channel region is highly disordered, but arranged in a tapelike planar fashion along the crystallographic *b* axis direction. If assigned as carbon atoms, most peaks refined to less than full occupancy. Two peaks refined to significantly greater than or near 100% carbon occupancy. These were assumed to be iodine atoms from the crystal soaking agent iodobenzene. Two independent, partially occupied C_6H_5I molecules were modeled. Both are further disordered about a crystallographic inversion center. The phenyl rings of each were fitted to rigid hexagons, and both bonded C-I distances were restrained to 2.10(1) Å. 1,3-C-I distances were restrained to be similar to each other (SHELX SADI). Occupancies refined to: I1S/C1S-C6S = 0.156(2) and I2S/C7S-C12S = 0.091(2), generating a C_6H_5I composition per cycle of 0.494(6). All non-hydrogen atoms were refined with anisotropic displacement parameters. All carbon atoms of the iodobenzene C_6 rings were assigned a common anisotropic displacement parameter. They were further restrained to approximate an isotropic shape (SHELX ISOR). Hydrogen atoms bonded to carbon were placed in geometrically idealized positions and included as riding atoms with *d*(C-H) = 0.95 Å and *U*iso(H) = 1.2*U*eq(C) for aromatic hydrogen atoms and *d*(C-H) = 0.99 Å and *U*iso(H) = 1.2*U*eq(C) for methylene hydrogen atoms. The two urea hydrogen atoms were refined isotropically with *d*(N-H) = 0.84(2) Å distance restraints. The largest residual electron density peak in the final difference map is 0.61 $e^-/Å^3$, located 0.71 Å from C1S.

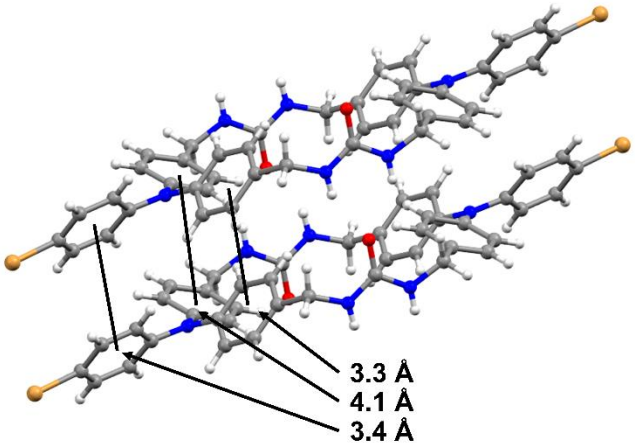

Figure S17. Crystal view of **1**·$(DME)_{0.5}$ showing the π-stacking in-between macrocycles. The three phenyl rings of the TPA unit align in an offset π-stacking arrangement with perpendicular distances of 3.2536(14), 3.4086(14), and 4.1013(15) Å.

Table S3. Comparison between different *bis*-urea macrocycles.

Macrocycle Spacer	Approximate Pore Size (Å)[a]	Void Space (% per unit cell)[b]	Urea Repeat Distance (Å)	Inter-columnar π-stacking
Benzene[7]	1.0 x 1.4	0	4.62	Offset π-stacking
Phenyl Ether[8]	4.5 x 6.7	14.5	4.65	Edge-to-face
Benzophenone[9]	5.0 x 7.1	14.9	4.72	Edge-to-face
4-Bromotriphenylamine	4.3 x 6.5	10.1	4.62	Offset π-stacking
m-di(phenylethynyl)benzene[10]	8.4 x 13.0	22.2	4.69	Alkyne phenyl stacking

[a]Calculated by measuring distance between diagonal hydrogens and opposing carbonyls and subtracting the *vdw* radii (See Fig. 3A). [b]Calculated by removing initial guest in channels and performing a contact surface void space calculation in Mercury (probe radius 1.2 Å, grid spacing 0.1 Å).[11]

Thermalgravimetric Analysis (TGA)

TGA was carried out using TA instruments SDT-Q600 simultaneous DTA/TGA at a rate of 3˚/min from 25-90˚C with a 5 minute isotherm before temperature increase and 150 minute isotherm after.

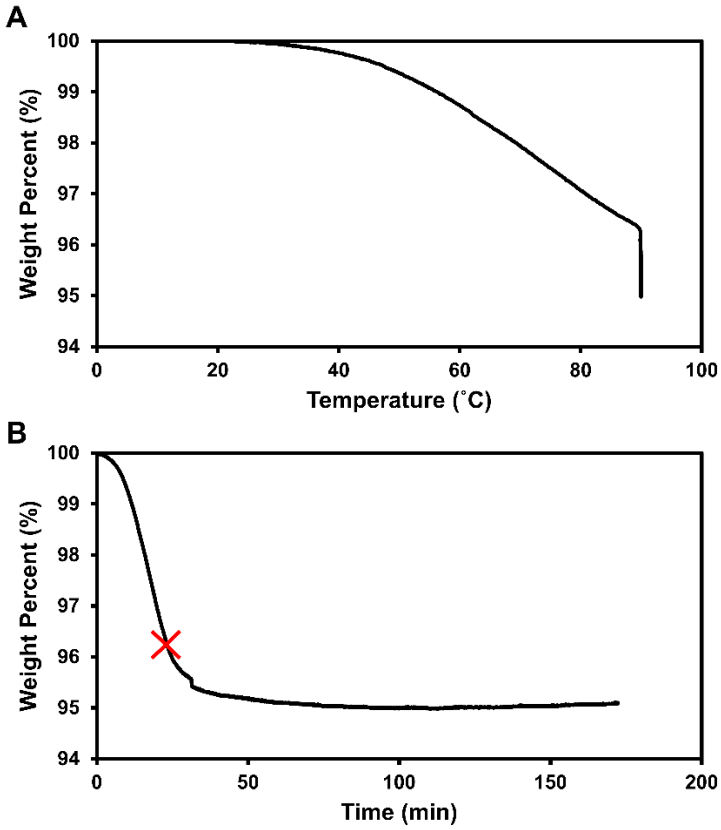

Figure S18. TGA graphs showing a one-step desorption of DME from **1**·$(DME)_{0.5}$. (A) Shows X-axis temperature and (B) shows x-axis as time (better indicator to ensure complete guest removal). Red X indicates where 150 minute isotherm at 90˚C began. Host: guest ratio calculated to be 1:0.5. An average of 1:0.55 was found from an average of three trials.

Hirshfeld calculations

The molecular Hirshfeld surface for **1** was constructed using Crystal Explorer 17.5.[12-16] The crystallographic information file (.cif) of **1**·$(DME)_{0.5}$ was imported into Crystal Explorer, and the guest (DME) was removed. Then a high resolution Hirshfeld surface was mapped with the d_{norm} function. A two dimensional fingerprint map was obtained by calculating the distances from the Hirshfeld surface to the nearest interior nucleus (d_i) to the outside surface (d_e) to measure interactions to neighboring molecules. The Hirshfeld surface was generated over a d_{norm} range of -0.5 to 1.5.

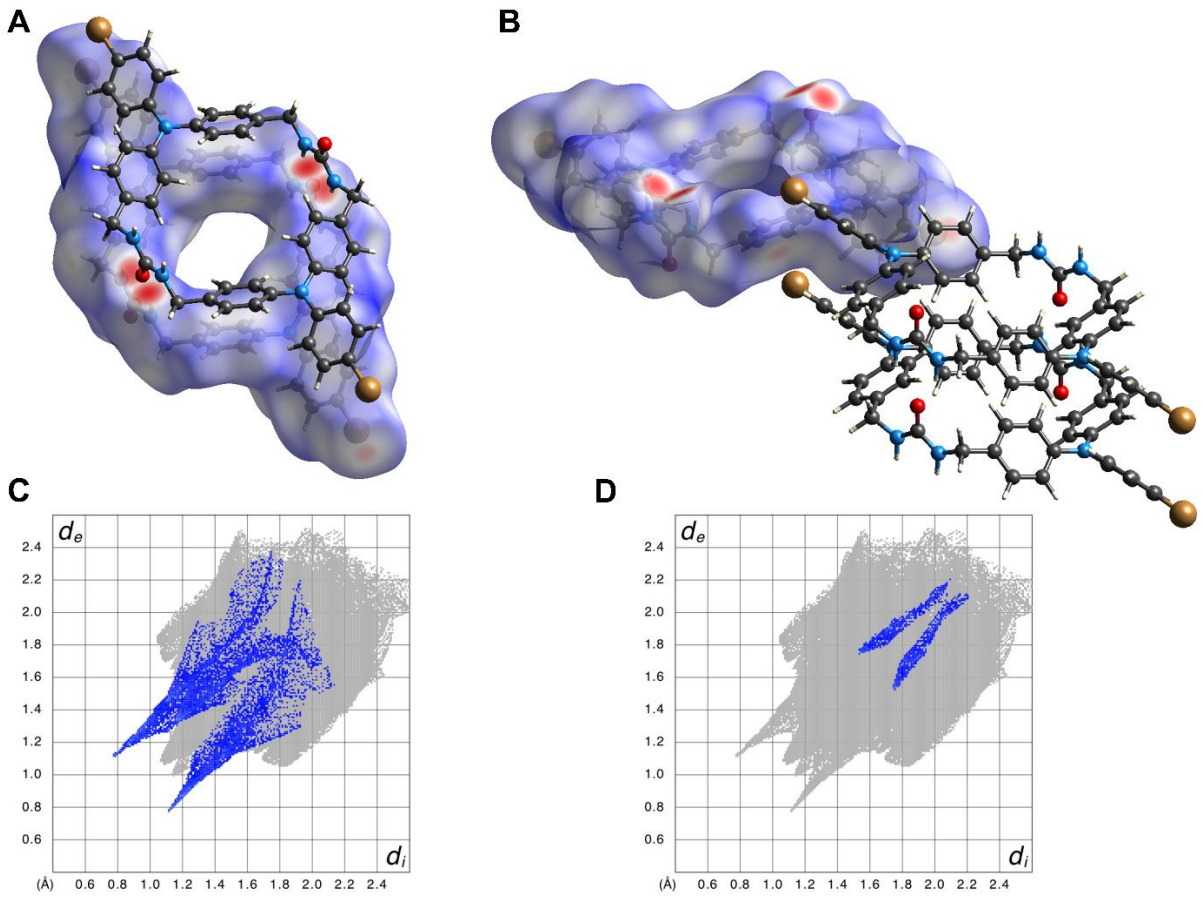

Figure S19. Hirshfeld surface analysis of macrocycle **1**. (A) Bifurcated hydrogen bonding between macrocycles. Red areas represent distances shorter than sum of the *vdw* radii while blue regions are longer. (B) Br···C_{aryl} interactions between neighbouring macrocycles. (C) Fingerprint plot resolved for O···H/H···O contacts. (D) Fingerprint plot resolved for Br···C/C···Br contacts.

Sample preparation for ^{129}Xe NMR measurements

A medium wall 5 mm NMR tube (Wilmad-Labglass) was loaded with around 100 mg of Br-TPA macrocycle and attached to a custom-built vacuum system. The sample was made sorbate free by exposing it to a high vacuum (< 10^{-4} bar) at 298 K for at least 10 hours. A desired quantity of ^{129}Xe gas (99% enrichment, Sigma-Aldrich) was cryogenically loaded into the tube using liquid nitrogen to achieve a loading pressure of 9.5 bar at 298 K. After loading, the tube was flame sealed and left to equilibrate at 298 K for at least 12 hours before NMR measurements.

^{129}Xe PFG NMR and relaxation measurements

^{129}Xe pulsed field gradient (PFG) NMR and ^{129}Xe NMR relaxation measurements were performed at 298 K using a wide-bore Avance III HD 17.6 T spectrometer (Bruker Biospin) operating at 208.6 MHz. The magnetic field gradients were generated using Diff50 diffusion probe and GREAT 60 gradient amplifier (Bruker Biospin). A standard stimulated echo PFG NMR sequence with the sine-shaped gradient pulses was used. The duration between the first and second radiofrequency pulses was 0.68 ms, and the diffusion time was varied between 5 and 100 ms. The gradient duration and maximum amplitude were equal to around 0.20 ms and 3 T/m, respectively. Using larger durations and amplitudes of the gradient pulses was not possible due to a relatively short transverse (T_2) NMR relaxation time of the strongest line of the adsorbed ^{129}Xe (around 0.4 ms). This short T_2 time also prevented an application of PFG NMR sequences with bipolar gradients, such as a 13-interval PFG NMR sequence.[17] The T_2 time was estimated using the stimulated echo sequence by changing the time intervals during which the T_2 NMR relaxation takes place. Longitudinal (T_1) NMR relaxation measurements of the adsorbed Xe were performed using a standard inversion recovery sequence. The T_1 time of the strongest line of the adsorbed ^{129}Xe was found to be around 7 s.

In the case of normal self-diffusion with a single diffusion coefficient (*D*), PFG NMR attenuation curves measured by the stimulated echo PFG NMR sequence can be presented as[18]

$$\Psi = \frac{S(g)}{S(g \approx 0)} = \exp(-Dq^2 t), \quad (1)$$

where Ψ is the PFG NMR signal attenuation, *S* is the PFG NMR signal intensity, *t* is the time of observation of diffusion process (i.e., diffusion time) and $q = \gamma g \delta$, where γ is the gyromagnetic ratio and δ is the effective gradient pulse length. Eq. (1) is expected to hold for the diffusion of Xe in the voids between porous particles as well as for long-range diffusion, i.e. diffusion under the conditions of fast exchange of Xe atoms between porous particles and the surrounding gas phase. In the complete analogy with gas diffusion in zeolite beds, the long-range diffusivity (D_{lr}) in the studied sample can be presented as[18]

$$D_{lr} = p_{\text{int}} D_{\text{int}}, \quad (2)$$

where p_{int} is a fraction of Xe atoms, which at any particular time are located in the voids between the porous particles, calculated with respect to all Xe atoms in a particle bed, and D_{int} is the diffusivity of Xe in the voids between porous particles. Eq. 2 is expected to provide a good approximation for the studied sample because the diffusion process in microporous particles is many orders of magnitude slower than that in the gas phase between the particles. The value of p_{int} was estimated to be ≥ 0.37 from the area under the ^{129}Xe NMR lines corresponding to the adsorbed and gas-phase Xe. Hence, $D_{lr} \geq 0.37\, D_{int}$. Using the measured value of D_{int} for Xe in the studied sample (6.7×10^{-7} m^2/s at 298 K) we estimate that the attenuation (Eq. 1) of the ^{129}Xe PFG NMR signal for the case of the long-range diffusion at the largest gradient used in this work should be ≤ 0.09. It is important to note that this is only an estimate. A complete analysis of the diffusion attenuation in the case of chemical exchange is provided, for example, in ref.[19] We observe that $\Psi = 1.0$ with the uncertainty of 20% in all cases for the line at 206 ppm, which is attributed

to Xe adsorbed in the channels. This observation rules out fast exchange of Xe atoms between the channels and the surrounding gas phase on the time scale used in the measurements (5-100 ms).

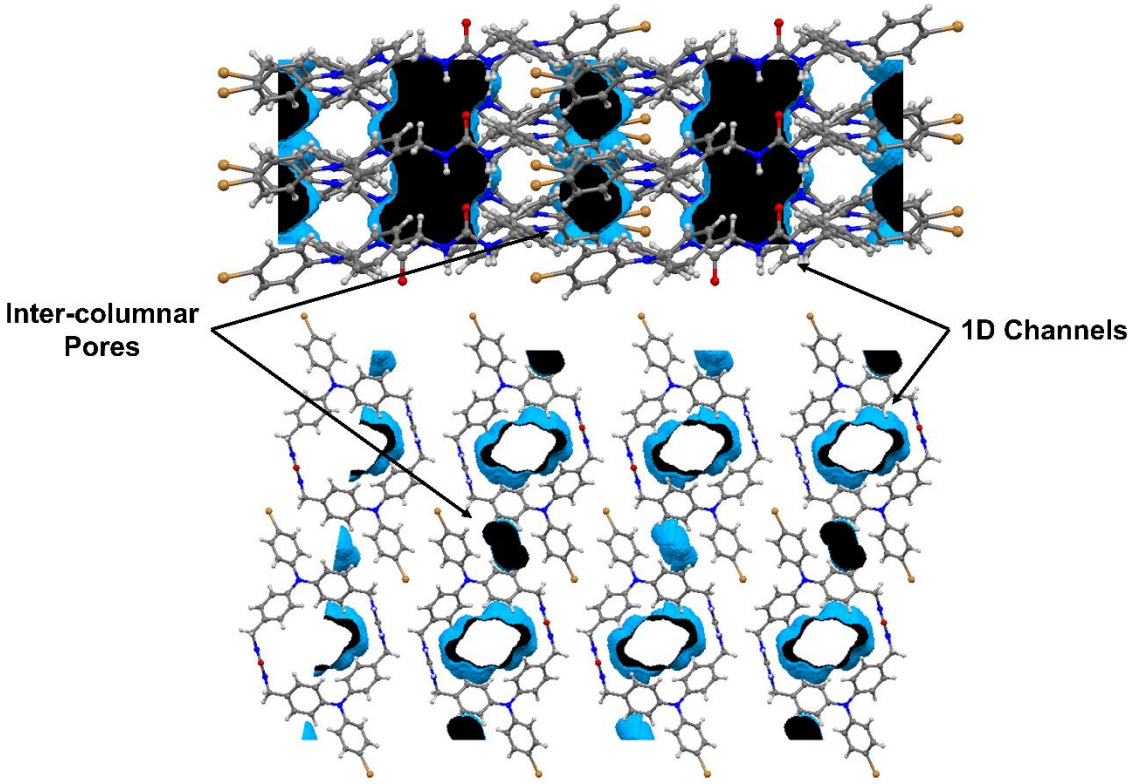

Figure S20. Views of **1** showing void space within columns. Top view is looking down *c* axis and bottom view is looking down *b* axis. Calculated by performing a contact surface void space calculation in Mercury (probe radius 0.9 Å, grid spacing 0.1 Å).[11]

References

1 G. K. Paul, J. Mwauru, A. A. Argun, P. Taranekar, and J. R. Reynolds, *Macromolecules*, 2006, **39**, 7789.

2 *APEX3 version 2016.5-0, SAINT + Version 8.37A*; Bruker AXS, INC.: Madison, WI, 2016.

3 SADABS-2016/2 L. Krause, R. Herbst-Irmer, G. M. Sheldrick, and D. Stalke, *J. Appl. Cryst.*, 2015, **48**, 3.

4 SHELXT G. M. Sheldrick, *Acta Crystallogr. A*, 2015, **A71**, 3.

5 SHELXL G. M. Sheldrick, *Acta Crystallogr. C*, 2015, **C71**, 3.

6 O. V. Dolomanov, L. J. Bourhis, R. J. Gildea, J. A. K. Howard, and H. Puschmann, *J. Appl. Crystallogr.*, 2009, **42**, 339.

7 L. S. Shimizu, M. D. Smith, A. D. Hughes, and K. D. Shimizu, *Chem. Commun.*, 2001, 1592.

8 L. S. Shimizu, A. D. Hughes, M. D. Smith, M. J. Davis, B. P. Zhang, H. zur Loye, and K. D. Shimizu, *J. Am. Chem. Soc.*, 2003, **125**, 14972.

9 M. B. Dewal, Y. Xu, J. Yang, F. Mohammed, M. D. Smith, and L. S. Shimizu, *Chem. Commun.*, 2008, 3909.

10 S. Dawn, M. B. Dewal, D. Sobransingh, M. C. Paderes, A. C. Wibowo, M. D. Smith, J. A. Krause, P. J. Pellechia, and L. S. Shimizu, *J. Am. Chem. Soc.*, 2011, **133**, 7025

11 C. F. Macrae, I. J. Bruno, J. A. Chisholm, P. R. Edgington, P. McCabe, E. Pidcock, L. Rodriguez-Monge, R. Taylor, J. van der Streek, and P. A. Wood, *J. Appl. Crystallogr.*, 2008, **41**. 466.

12 F. L. Hirshfeld, *Theor. Chim. Acta*, 1977, **44**, 129.

13 M. A. Spackman and D. Jayatilaka, *CrystEngComm*, 2009, **11**, 19.

14 J. J. McKinnon, D. Jayatilaka, and M. A. Spackman, *Chem. Commun.*, 2007, 3814.

15 S. K. Wolff, D. J. Grimwood, J. J. McKinnon, M. J. Turner, D. Jayatilaka, and M. A. Spackman, *CrystalExplorer (Version 3.1)*, University of Western Australia, 2012.

16 M. A. Spackman and J. J. McKinnon, CrystEngComm, 2002, **4**, 378.

17 R. M. Cotts, M. J. R. Hoch, T. Sun, and J. T. Markert, *J. Magn. Reson.*, 1989, **83**, 252.

18 J. Kärger, D. M. Ruthven, and D. N. Theodorou, *Diffusion in Nanoporous Materials*, Wiley-VCH, Weinheim, 2012.

19 E. D. Hazelbaker, S. Budhathoki, H. Wang, J. Shah, E. J. Maginn, and S. Vasenkov, *J. Phys. Chem. Lett.*, 2014, **5**, 1766.